Article

Modelling Water Erosion and Mass Movements (Wet) by Using GIS-Based Multi-Hazard Susceptibility Assessment Approaches: A Case Study—Kratovska Reka Catchment (North Macedonia)

Bojana Aleksova [1], Tin Lukić [2,*], Ivica Milevski [1], Velibor Spalević [3] and Slobodan B. Marković [2,4]

[1] Institute of Geography, Faculty of Natural Sciences and Mathematics, Ss. Cyril and Methodius University, Arhimedova 3, 1000 Skopje, North Macedonia; aleksova_bojana@yahoo.com (B.A.); ivica@pmf.ukim.mk (I.M.)

[2] Department of Geography, Tourism and Hotel Management, Faculty of Sciences, University of Novi Sad, Trg Dositeja Obradovića 3, 21000 Novi Sad, Serbia; slobodan.markovic@dgt.uns.ac.rs

[3] Biotechnical Faculty, University of Montenegro, Mihaila Lalića 15, 81000 Podgorica, Montenegro; velibor.spalevic@ucg.ac.me

[4] Serbian Academy of Sciences and Arts, Kneza Mihaila 35, 11000 Belgrade, Serbia

* Correspondence: tin.lukic@dgt.uns.ac.rs

Abstract: Kratovska Reka is a short (17.3 km) left tributary of Kriva Reka, whose watershed (68.5 km^2) is located on the northwestern slopes of the Osogovo Mountains (North Macedonia). Due to the favorable natural conditions and anthropogenic factors, the Kratovska Reka catchment is under a high risk of natural hazards, especially water erosion and landslide occurrences. For this reason, the paper presents an approach of modelling of potential erosion and areas susceptible to the above-mentioned hydro-meteorological hazards in the Kratovska River catchment. Firstly, this study analyzed the main geographical features that contribute to intensive erosion processes in the area. Then, using the Gavrilović EPM erosion potential method, an average value of 0.56 was obtained for the erosion coefficient Z, indicating areas prone to high erosion risk. Furthermore, by using landslide susceptibility analysis (LSA), terrains susceptible to landslides were identified. The results shows that 1/3 of the catchment is very susceptible to mass movements in wet conditions (landslides). According to the combined multi-hazard model, 3.13% of the total area of the Kratovska River catchment is both at high risk of landslides and under severe erosion. The Kratovska River catchment is significantly endangered by the excessive water erosion processes (39.86%), especially on the steep valley sides, i.e., terrains that are completely exposed, under sparse vegetation, and open to the effects of distribution/concentration of the rainfall amounts throughout the year. Identifying locations with the highest erosion risk serves as the initial step in defining and implementing appropriate mitigation measures across local and regional scales, thus enhancing overall resilience to environmental challenges.

Keywords: hydro-meteorological hazards; water erosion; mass movement (wet); multi-hazard modelling; GIS; risk assessment; geohazard mitigation; watershed; Kratovska Reka; North Macedonia

1. Introduction

Phenomena or events that degrade the quality of the environment and have a potential for endangering people, property, and infrastructure are called geohazards [1]. Based on the literature findings, geohazards have a significant impact on human health and economic development, leading to consequences such as human casualties [2–5], direct damage to infrastructure or private property [6,7], a negative impact on household income [8,9], alteration of consumer behavior among various income groups [10,11], and lower life satisfaction [12–14]. For the most part, geohazards are generated as a result of a combination

of unfavorable natural factors and, in certain situations, they can also be caused by humans. Refs. [15,16], through examples, explain that geohazards have a negative impact on geosites.

Until a few decades ago, natural and geohazards were considered to be typically natural, i.e., occurring naturally. However, recently, it has been realized that anthropogenic factors have an increasing direct or indirect impact on their occurrence and frequency [17]. That is why the expression "anthropogenic–natural disasters" or "anthropo-geohazards" is used more frequently worldwide today. As noted by [18], during the last several decades, Europe has predominantly experienced hydro-meteorological hazards that frequently give rise to diverse risk factors, including environmental changes, population dynamics, infrastructure vulnerabilities, and socio-economic aspects [19–21].

In terms of climate-related risks, South-Eastern Europe (SEE) could be identified as one of the world's critical areas [22]. This geographical area has been known for its numerous hydro-meteorological hazards throughout modern history [23]. These undesirable natural events often cause environmental, social and, therefore, economic damage, with long-term consequences, and can easily turn into disasters with catastrophically large effects. The severity of economic damage can be illustrated by the reported loss of over EUR 433 billion for the period 1980–2015 in the European Economic Area [24]. With an evidently increasing number of extreme weather events induced by climate change, hydro-meteorological hazards have emerged as a high-impact risk, especially in Europe [25–27]. Contemporary research in the field [24] has presented unfortunate facts related to hydro-meteorological hazards in Europe. All major hazardous events (heavy precipitation episodes/floods, storms, landslides/rockfalls, wildfires, droughts, extreme temperatures) have increased in frequency and/or intensity. Projected scenarios for the future are not optimistic, since even more natural hazard-related damage is expected for various sectors [25]. During these hazardous events, humans, and anthropogenic systems in general, are highly exposed and vulnerable [28]. Climate and weather conditions are not the only reason for this. As the global population continues to experience a rising trend (estimated to be 11 billion by the end of this century), (United Nations-UN), accompanied by urbanization of natural disaster-prone zones [29], society development and economic growth [30], the amplification of natural hazards impact is imminent. This socio-economic development has also led to tourism expansion, thus increasing its sensitivity to weather-related hazards [18].

In the last few decades, there has been great interest in analyzing and assessing the risk of natural hazards and geohazards. The huge interest is the result of a large number of casualties and the damage caused by these natural hazards around the world [31–37]. According to [38], the acceleration of the process of soil erosion can cause a potential problem for agriculture. Soil erosion may be doubled with an increase in slope and relative angle of terrain [39–41]. As pointed out by [42], the Western Balkans region is highly prone to water erosion processes and, therefore, the estimation of rainfall erosivity potential is essential for understanding the complex relationships between hydro-meteorological factors, soil erosion processes and main topographical features.

According to [2,43], this has led to the development of various simulation models of different accuracy and complexity, including empirical, stochastic, and deterministic models. Additionally, indicators based on biological, physical, social, and economic approaches have also been utilized. Empirical models are commonly used, particularly in countries where input data are often limited, and their validity is uncertain, such as Western Balkan and southeastern European countries. These models are preferred due to their simplicity and ease of use, having less input data and fewer computations, compared to more comprehensive models [43].

Ref. [43] conducted a study evaluating soil erosion and its spatial distribution using two empirical models, namely the erosion potential model (EPM), also known as the Gavrilović method, and the RUSLE model. The study focused on the Venetikos River catchment, the largest tributary of Aliakmonas River, located in northern Greece. Both models demonstrated a satisfactory simulation of the phenomenon, exhibiting acceptable precision and enabling the identification of areas most susceptible to erosion and land

degradation. Although both models performed quite similarly and attributed underestimated results in comparison to the "actual" (measured) values of mean annual sediment discharge and yield, the EPM approach was used in the study to generate comparable data with neighboring countries where the same approach was applied [44–46].

The EPM model has been extensively implemented across the Balkans and in other countries worldwide, including Serbia, Croatia, Slovenia, Germany, Italy, Argentina, Belgium, and Greece [43–48]. Its application has provided reliable results for assessing water erosion severity, estimating mean annual soil loss and sediment yield, and implementing erosion control measures and torrent regulation at a regional scale.

Due to very favorable natural conditions as well as the human impact over the centuries, the territory of North Macedonia is highly exposed to various natural hazards [17,49], and geohazards [50]. Among the most dominant geohazards in this area are excessive erosion, torrents, landslides, rockfalls, floods, etc. [49]. Such phenomena, to a lesser extent, have also been recorded in the Kratovska Reka catchment, which is the case study in this paper. The main reasons for this are steep slopes and extensive areas covered with erodible crystalline rocks and tuffs, combined with high human impact and deforestation occurring over centuries. For those reasons, there are many sites in the catchment with severe erosion, especially along the banks and steep valley sides, with occasional threats to property and people's lives. Landslides are frequent as well, especially those that cause material damage, and destruction of roads (for example, the Kratovo—Probištip road), buildings, etc.

Only a few studies of geohazards in this area have previously been carried out [50–54]. However, most of these studies cover larger (regional to national) areas and only briefly mention the high erosivity and landslide susceptibility in the Kriva Reka catchment, without detailed analyses.

Because of the worldwide increased threat of geohazards, new methods are being developed to access or to perform a zonation of endangered areas, especially considering landslides, flashfloods, excess erosion, etc.

According to UNDRR, the multi-hazard concept refers to the selection of multiple major hazards that an area faces and the specific contexts in which hazardous events may occur simultaneously, cascadingly, or cumulatively over time, taking into account the potential interrelated effects.

Multi-hazard techniques are very important for the analysis of hazardous events [55–60]. Another approach could be achieved by implementing probabilistic and deterministic stochastic processes [61].

Accordingly, there is a need to develop models for the potential erosion and landslide susceptibility areas in the Kratovska Reka catchment. Therefore, the main objectives of this study are to: (1) perform multi-hazard assessment (hydro-meteorological hazards) in the study area by applying a modified erosion assessment model and joint systematic approaches; (2) produce hazard risk and susceptibility maps, and (3) identify places of greatest erosion risks as the starting point for defining and implementing suitable mitigation measures.

2. Data and Methodology

2.1. Study Area (Kratovska Reka Catchment, North Macedonia)

Kratovska Reka flows in the northeastern part of North Macedonia and passes through the city of Kratovo, where it is arranged with a concrete channel (built between 2015 and 2020) (Figure 1). The river source is on Osogovo Mountain at 1366 m (Lisec locality), while the inflow in Kriva Reka is at 412 m, thus, the total fall is 954 m. The length of the river is 17.3 km, and the catchment area covers 68.5 km^2.

The valley of Kratovska Reka is generally incised in volcanic rocks that dominate this area. The gorge-like valley has an average depth of 400–500 m and steep sides.
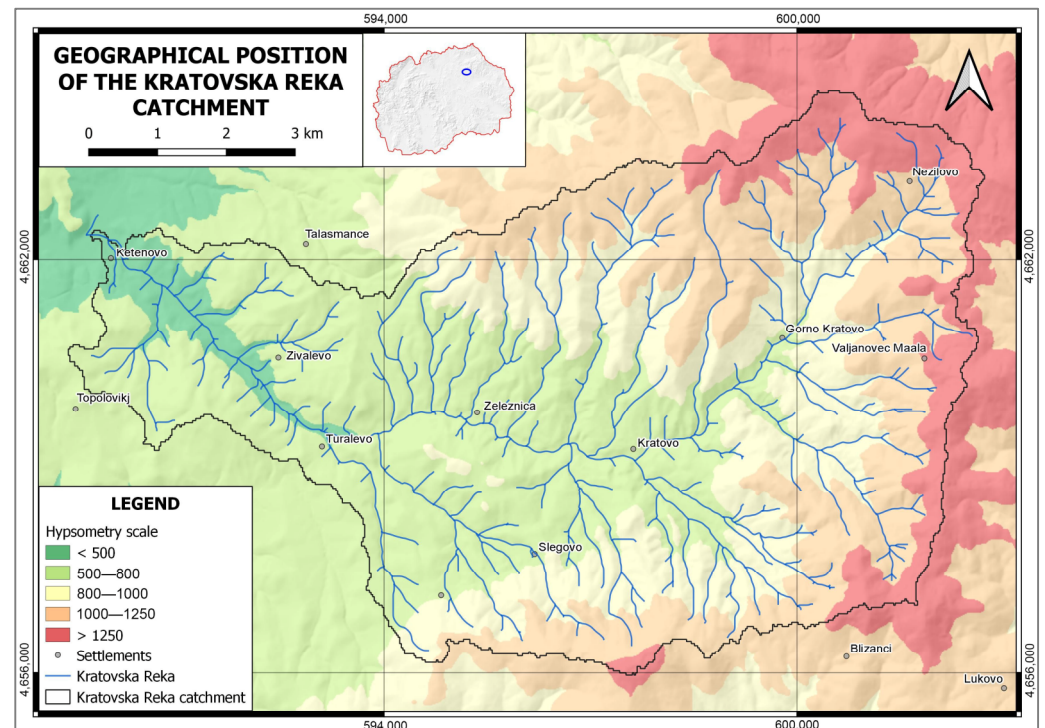
Figure 1. The geographical position of the Kratovska Reka catchment.

The lithology of the Kratovska Reka catchment is quite complex, represented mainly by Precambrian and Paleozoic crystalline rocks that are intruded and covered by younger intrusive and effusive magmatites [62] (Figure 2, left side). Overall, rock masses with high erodibility (tuffs, shists, clastic sediments, breccia, etc.) dominate, at 51.7%. They are easily susceptible to weathering, decomposition, and washing, which is the reason for the strong erosion processes in the Kratovska Reka catchment.
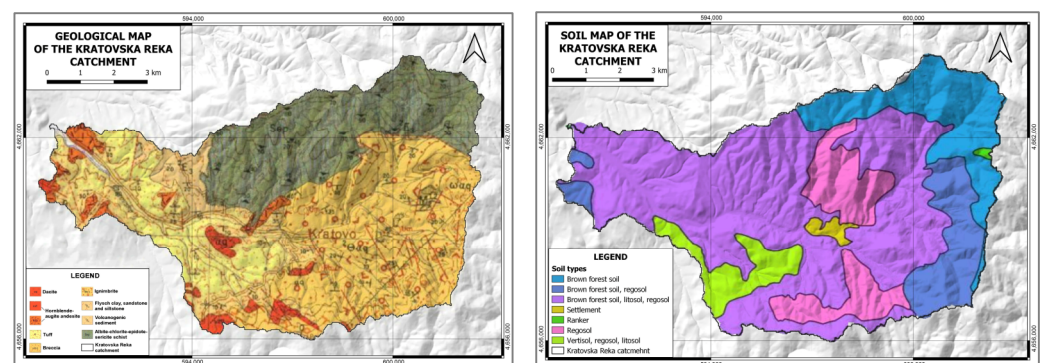

Figure 2. Left: Geological map of the Kratovska Reka catchment (according to [62]). **Right**: soil map of the area (according to [63]).

In the Kratovska Reka catchment, soil types that are the result of strong water–mechanical erosion and accumulation are widespread, especially on steep, hilly terrains with sparse vegetation. According to the National Soil Map at a scale of 200 k [63], the study area is primarily dominated by cambisols, leptosols, regosols, and vertisols (Table 1).

These soil types are relatively shallow and predominantly cover volcanic rocks and schists in the underlying strata. However, it is important to acknowledge the limited availability of soil data and soil profiles for the catchment area, resulting in a soil map of poor quality for this region. Through field observations, it becomes apparent that the soils in the hilly–mountainous terrains are weakly developed and subject to significant

erosion. In the narrow valley bottom of Kratovska Reka, downstream of Kratovo, fluvisols are also present. These soils are primarily sandy and contain a notable proportion of river sediments, such as gravel and pebbles.

Table 1. Main physical properties of the soils in the Kratovska Reka catchment (according to [64]).

WRB Classification of the Soil Type	Soil Texture Type	Clay Content in %	Structure	CaCO$_3$ Content in %
Cambisol (brown forest soil)	Sandy loam or finer	8	ABC	0
Leptosol	Shallow soils lacking well-defined horizons	0	(A)-R	0
Regosol	Shallow, medium—to fine-textured	15	(A)-C	13.44%
Vertisol	Clay-rich soils	65	A-AC-C-(R)	0
Ranker	Lithomorphic soils	5	A-AC-C-R	0
Fluvisol	Heavy clays in the catchment area	10	(A)-(Ah)-C	0

In terms of topography, the catchment elevation ranges from 412 m to 1550 m, while 66.1% of the area is below 1000 m, where the human impact is strongest. However, the terrain slope has the highest impact on the erosion and landslide processes in the Kratovska Reka catchment. According to the 15 m DEM, 15.6% of the catchment has steep slopes (>30°), while the mean slope is 20.9°. The plains or terrain with slopes bellow 3° cover only 1.3%, showing that the entire area is highly inclined. Hillslopes generally have western, and south-western (adjacent) aspects, which favorably reflect on the erosion intensity. In the Kratovska Reka valley, it has been observed that the weathering of dacite–andesite rocks occur predominantly on the southern or western exposures, and much less on the northern sides.

Terrain relief is in the range of 34.3–243.1 m/km^2, with a mean value of 105.4 m/km^2. Terrain with an elevation difference of between 150–300 m/km^2 covers 8.3% of the catchment. This means that, the higher the topographic ruggedness index, the greater the danger of geohazards (erosion, landslides) (Figure 3).
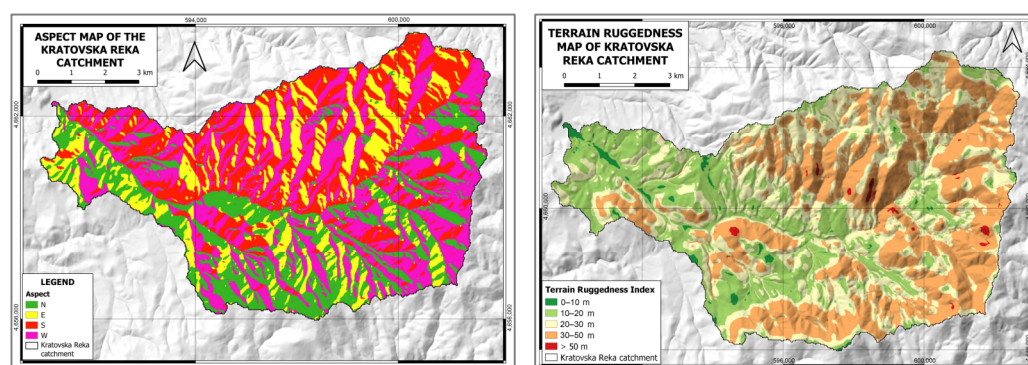

Figure 3. Aspect map (**left**), and terrain ruggedness map in meters (m) (**right**).

According to [65], the climate is generally moderate–continental with an average annual temperature of 11.4 °C, ranging from a mean of 21.4 °C in August to 0.4 °C in January. The average annual precipitation is relatively low (728.4 mm), with the maximums in May (84.9 mm), and November (69.6 mm), and the minimum in August (35.1 mm). Of the total average annual amount, 57% falls in the vegetation period, 28% in the spring months, 22% in the summer, 24% in the autumn, and 26% in the winter. Of the total annual average number of days with precipitation (97), only 9% have a daily amount equal to or

greater than 20.0 mm, reaching up to 110 mm/day [58]. During winter, the upper section of the catchment is typically covered in snow, which can swiftly melt as spring arrives. Intense rainfall, prolonged precipitation episodes, and rapid snowmelt contribute to significant overland flow and severe erosion in exposed or poorly protected areas. The main features of the climate are presented in Figure 4.
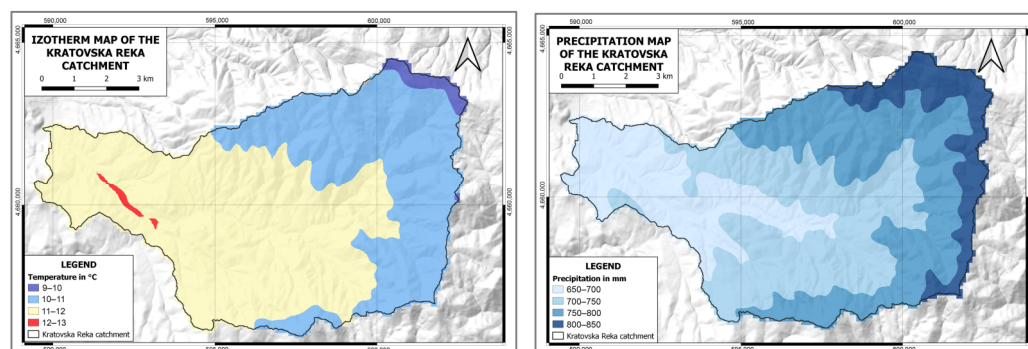

Figure 4. Isotherm map (**left**), and precipitation map (**right**) of the study area.

Closely connected with the previous factors, especially climate, is the hydrography of the area, with the most important hydrographic features presented in Table 2.

Table 2. Characteristics of the river network in the Kratovska Reka catchment (P = area, N = number of tributaries, L = length of all tributaries, D = density of river network in km/km^2), Hmm = average annual precipitation, Qsr = average flow, H-a m = mean height of the catchment, Hvl m = estuary altitude, ΔHs-v = mean height difference of the catchment, Lc = length of the catchment, Lw = length of the watershed, α^o av. = average drop of the watershed, AC = coefficient of asymmetry).

Watershed	P km^2	N	L km	N/P	D	Hmm	Qsr m^3	H-a m	Hvl m	ΔHs-v	Lc km	Lw km	α^o av.	AC
Kratovska Reka	68.5	20	98.4	0.5	2.0	701	0.6	879	406	473	17.3	17.4	21.0	1.5

The presence or absence of vegetation cover is a crucial factor contributing to erosion processes in the investigated area. According to the [66] CORINE Land Cover 2018 (CLC2018) map, the largest area of the catchment is covered by discontinuous urban fabric (36.3%). Non-irrigated arable land occupies 20.7%, pastures 15.9%, and complex cultivation patterns 15.7% of the total area. Forests in the area are predominantly situated at altitudes above 1000 m, with broad-leaved forest, mixed forest, transitional woodland–shrub, and bare soils below. The CLC2018 model shows a significant reduction in forest areas compared to CLC2000, probably due to logging.

The Kratovska Reka catchment completely belongs to the municipality of Kratovo. According to the last census of 2021 [67], the municipality of Kratovo has 7545 inhabitants, which is significantly less than the population from the census in 2002 (10,441 inhabitants). Thus, this is a typical depopulation area. In this sense, in the past centuries, there has been a much higher human impact on the landscape, not only by the larger population (concentrated in the hilly villages), but also by extensive agricultural activities.

2.2. Methodology for Erosion Assessment

For erosion assessment, the erosion potential model (EPM), also known as the Gavrilović method, is widely used in the majority of southeastern European countries, both at regional and national scales. This model was developed in the 1960s, based on erosion field research conducted in the Morava River catchment area (Serbia). The model includes erosion mapping, estimation of sediment quantities, and classification of torrential flooding [68]. As reported by [69] this method is convenient for areas with limited data derived from

previous erosion research, but it does not extensively delve into the underlying physics of the erosion processes.

In North Macedonia, similarly to other countries in the region, the estimation of average erosion potential and sediment yield is commonly accomplished using the EPM [70]. The method is based on the following equation:

$$Wy = T \cdot H \cdot 3.14 \cdot sqrtZ^3 \cdot f$$

where: W is the average annual amount of erosive material in m^3; T is a temperature coefficient in the form: T = (0.1 · t + 0.1) 0.5, where t is the annual mean air temperature; H indicates annual precipitation in mm; Z is the erosion coefficient ranging from 0.1 to 1.5 and above; and f is the studied area in km^2. Among these factors, the coefficient Z has the highest importance in combining rock erodibility/erosion resistance (Y), land cover index (Xa), index of visible erosion processes (φ), and mean slope of the catchment (J) in the ratio:

$$Z = Y \cdot Xa \cdot (\varphi + sqrtJ^{0.5})$$

According to the available data, in our GIS-based approach, appropriate digital layers are prepared, and the calculation of the erosion potential model (EPM) (e.g., [71,72], see Figure 5) involves the following procedures:
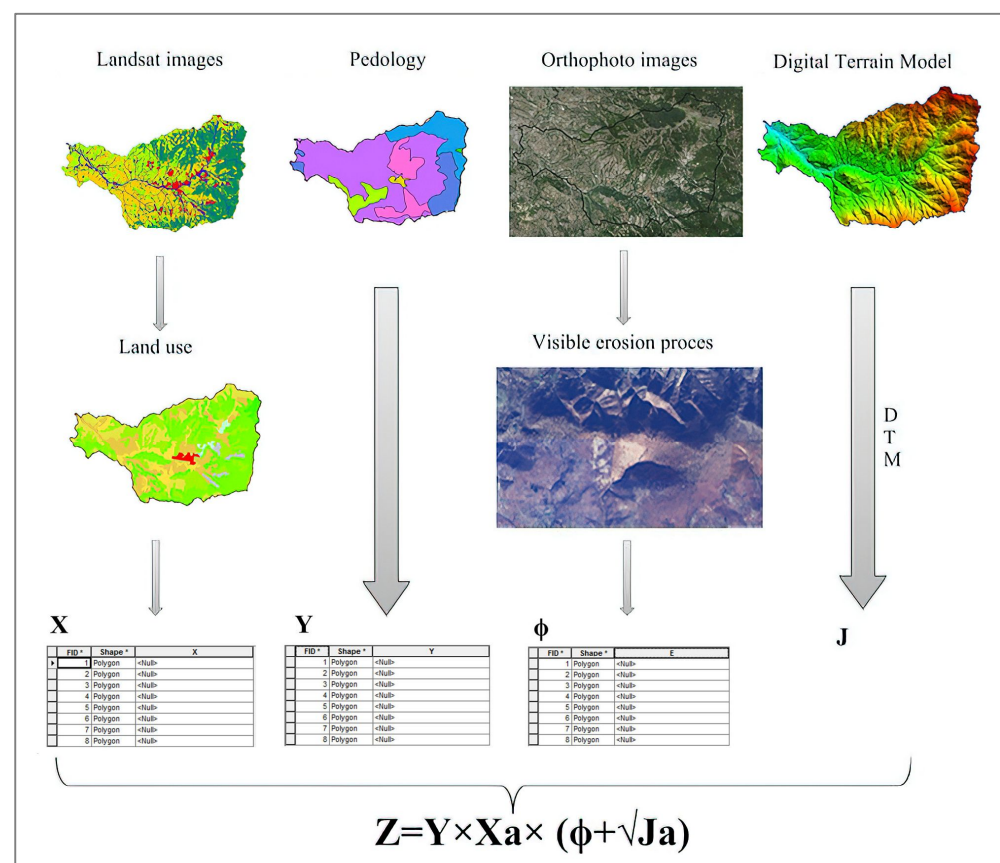

Figure 5. A schematic representation illustrating the calculation of the EPM using GIS-based methodology.

- Processing Landsat 8 satellite images (Table 3) from 2010 and 2020 (cloud-free images are used from the months of May (vegetation period), August (dry period) and October (the fall)), which includes supervised classification into six classes (populated areas, water bodies, surface mines, forests, low vegetation, industry, and transportation). This step results in obtaining vector maps of land use, used for the parameter Xa;

Table 3. Different spectral channels of Landsat 8 satellite images.

Band	Wavelength (φm)	Resolution (m)
Band 1	0.43–0.45	30
Band 2	0.45–0.51	30
Band 3	0.53–0.59	30
Band 4	0.64–0.67	30
Band 5	0.85–0.88	30
Band 6	1.57–1.65	30
Band 7	2.11–2.29	30

- Treatment of land maps based on the available soil folders, considering the recent situation of soil types and supplementing them with real-time information derived from the processing of Landsat 8 satellite images. This includes supervised classification and the separation of surface open pits, which are considered as areas of disturbed soil layers. This step provides the parameter Y;
- Determination of visible erosion processes through the analysis of orthophoto images, contributing to the calculation of the erosion coefficient φ;
- Creation of a digital terrain model (DTM) according to [73], where DTM serves as the basis for calculating the slope factor J_a.

Z values typically range between 0 (no erosion) and 1.5 (higher amount of erosion). Unlike traditional cartographic tools, the GIS approach in erosion potential model (EPM) implementation relies heavily on deriving most of its model parameters from the digital elevation model and satellite images [71,74–79].

Thus, for the Y coefficient, a previously prepared and digitized 100 k geological and soil map was used and then rasterized to 15 m. Notably, these maps were the most detailed available for the survey area and were also considered highly accurate. The given raster values correspond to the rock erodibility and erosion resistance values, according to the method proposed by Gavrilović [68]. Generally, the values range from 0.1 (very resistant rocks) to 2.0 (non-resistant rocks) [50]. However, due to the challenges associated with accurately estimating erodibility correlations [80], the fitting of the values is accomplished through a process known as double rooting in the form: Y = sqrt (Y1). The land cover index, X*a, is prepared from the CORINE Land Cover model (CLC2018), with values ranging from 0.1 (dense forests) to 1.0 (bare rocks). Relevant values are incorporated into the CORINE Land Cover (CLC) classes based on the suggested values from the original model [50].

In order to determine the value of the coefficient φ for visible erosion processes, the traditional model's subjective assessment is replaced with the utilization of Landsat 8 band 4 (b4-red). This involves dividing the grayscale values (ranging from 0 to 255) by 255. This is because this specific band consists of 255 shades of grey, where lower values indicate areas without visible erosion processes, while values closer to 255 indicate areas with excessive sheet, rill, and gully erosion. However, higher values may also indicate the presence of light anthropogenic structures, uncovered rocks, waste disposal sites etc. [50,70,79]. To address this issue, a correction is applied using the slope (a-in degree) in the form: φ = ((b4/255)*log(a + 1)), which leads to significantly more accurate values for the coefficient φ.

The slope factor (J) is computed using the available 15 m digital elevation model (DEM) as a raster layer representing the slope angle in radians (a = a/57.3). Following these steps, the GIS-calibrated coefficient Z is calculated using the equation:

$$Z = \text{sqrt}(Y)*\varphi*((X*a + \varphi)*\log(a +1) + \text{sqrt}(a/57.3)).$$

The main climate parameters in the model, such as the air temperature coefficient (T) and average annual precipitation (H), are determined using ERA5 average monthly data for

precipitation and air temperature, as well as MODIS land surface temperature (LST). These data are accessed and exported through the Google Earth Engine (GEE) script, covering the period from 1 January 2000 to 31 December 2022. The resulting raster models (grids) of average air temperatures and precipitation for the Kratovska Reka catchment serve as the basis for the T and H coefficients in the erosion potential model (EPM). Simultaneously, the accuracy of both models is verified using real measurement data from the Kratovo meteorological station, demonstrating a high level of accuracy, at 98.5%.

With the availability of air temperature and precipitation models, along with an erosion coefficient (Z) model, the mean annual erosion loss (Wy) for the entire catchment is calculated.

The GIS-based EPM approach has been previously tested in various regions and watersheds in North Macedonia [70,81], as well as in other countries [44,80,82–90]. Evaluation of EPM accuracy is generally performed by comparing the results with measuring the quantity the sediment deposition in the reservoirs [85,88,90], demonstrating strong correlations with both, measured and observed data.

2.3. Methodology for Landslide Susceptibility Assessment (LSA)

Modelling and mapping landslide-prone areas on a regional scale is a very complex task, because of many natural and anthropogenic factors related to landslide processes. For that reason, the results of landslide susceptibility assessment (LSA) from previous research on similar sized (test) areas were also included [49,91,92]. Furthermore, the work of [93] highlights the importance of evaluating six key triggering factors that significantly impact landslide activity. These factors include lithology, slope angle, land cover, terrain curvature, distance from rivers, and distance from roads.

The identification of influencing factors was the basis of several methods of LSA [94]. In a related study [95], these factors were categorized into two main groups, internal and external factors. The internal category encompasses mechanisms occurring within the mass that lead to a decrease in its shear strength below the external forces exerted on the mass by its surroundings, thereby inducing failure. On the other hand, the external category comprises mechanisms external to the mass that surpass its internal shear strength, consequently resulting in failure. According to [96], depending on the specific characteristics of the study area, it is essential to include at least three factors in GIS analysis, topography, lithology, and land use. These factors play a crucial role in assessing and modelling various aspects of the study area's multi-hazard susceptibility to specific processes. According to [97], the most frequently encountered conditioning factors are lithological units, tectonic features, slope angle, proximity to road or drainage networks, land cover, and rainfall distribution (concentration). Nonetheless, it is worth noting that there may be other factors that could be equally influential in certain contexts, even though they may not be as commonly considered.

In this research, six causative factors were taken into consideration: lithology, slope, plan curvature, land use, distance from streams, and distance from roads (Table 4; Figure 6). The selection of these parameters was based on the nature of the study area, the scale of analysis, and data availability [50]. For the slope and plan curvature data, a 15 m digital elevation model (DEM) of the entire catchment was used, and SAGA GIS software was employed to derive these variables. The lithology information was obtained from a digitalized and rasterized geological map of the town of Kratovo, at a scale of 100 k. This lithology map was then prepared within the Kratovska Reka catchment using QGIS software. It included nine lithological units, ranging from Precambrian schist to Cenozoic solid volcanic formations, Miocene dacitic ignimbrites, Pliocene andesites, tuffs, and Quaternary clastic sediments. The land use layer was created based on the CORINE Land Cover (CLC2018) classification hierarchy. Distance from streams was determined using the topographic river network (25 k) provided by the State Agency of Cadaster. Distance from roads was obtained from the OpenStreetMap (OSM) road network in vector (.shp) format. In the following steps, five buffer zones were established for both roads and streams, with increments of

20 m. These buffer zones were then converted into raster format. Finally, all the layers, including lithology, slope, plan curvature, land use, distance from streams, and distance from roads, were converted into a raster grid format with cell sizes of 15×15 m.

Table 4. Spatial data layers used in this study.

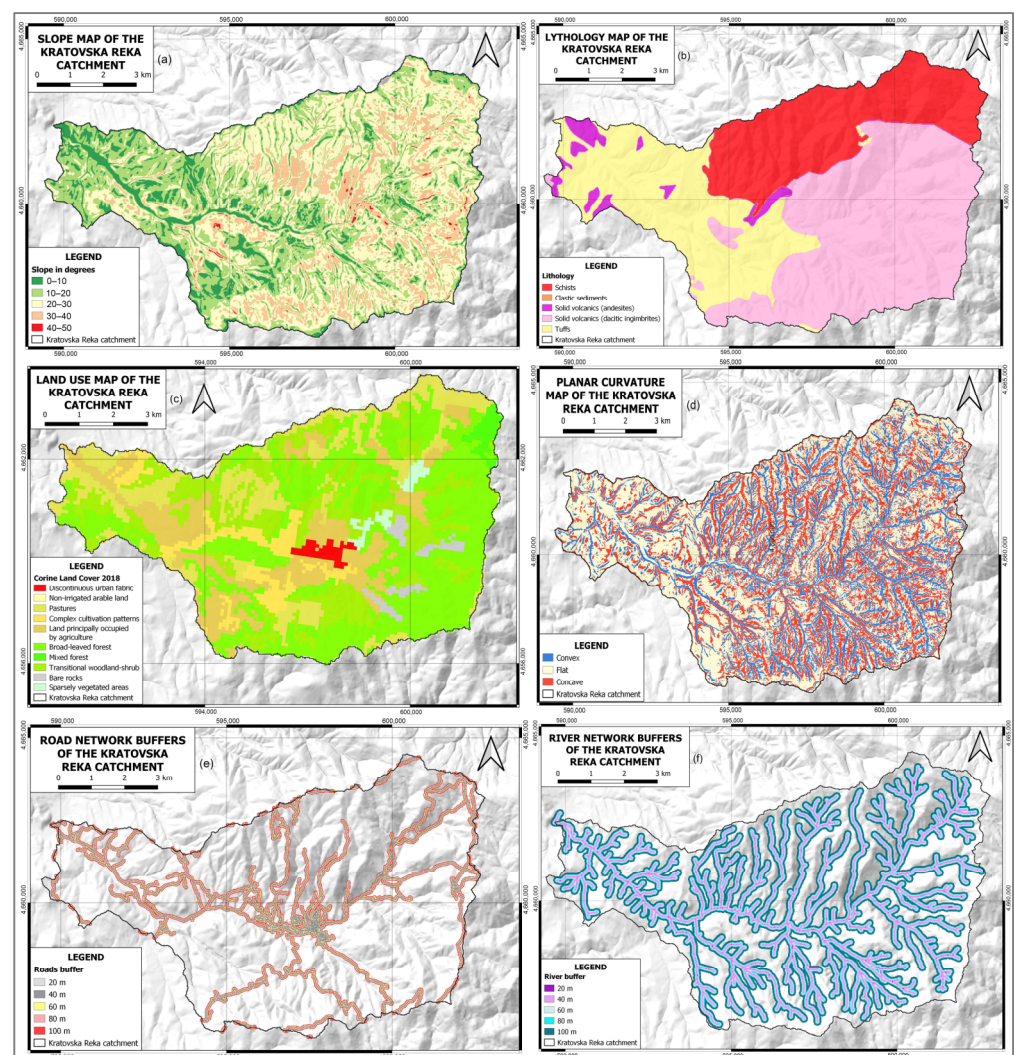| Factor-Layer	Source	Data Type
Slope, Planar curvature	15-m DEM	Grid (GeoTIFF)
Lithology	Digital geologic map	Grid (GeoTIFF)
Land use	CLC-2018	Grid (GeoTIFF)
Distance from stream	Topographic vector database	Line (shp)
Distance from roads	OSM roads database	Line (shp)

Figure 6. Raster layers of selected landslide-causal factors: (**a**) Slope, (**b**) Lithology, (**c**) Land cover, (**d**) Planar curvature, (**e**) Road network buffers, (**f**) River network buffers.

Following the previous steps, the next crucial stage involves selecting an appropriate LS (landslide susceptibility) method. In cases where the study area is extensive and lacks a comprehensive landslide inventory, statistical analysis of landslides and frequency ratio methods are considered highly effective. This approach relies on examining the correlation between the spatial distribution of landslides and each conditioning parameter. By assessing the relationship between landslides and these parameters, the LS method can be determined and implemented accordingly [98]. In this study, the relationship between

landslide occurrence and the selected conditioning factors (such as slope, lithology, land cover, etc.) is assessed through the calculation of the landslide susceptibility index (LSI). The LSI method involves calculating the index for each category within the chosen factors. This allows for the estimation of the susceptibility of each category to landslides based on their respective characteristics. According to [50], the analysis of LSA (landslide sensitivity analysis) is employed to assess the significance of different variables or changes in relation to landslide occurrences. Weighting factors are determined to evaluate the influence of each variable. These weighting factors compare the calculated density of landslides with the overall density of landslides in the study area. This comparison helps determine the relative importance of each variable in relation to landslide susceptibility [99]. It can be expressed as:

$$W_{ij} = 1000\left(f_{ij} - f\right) = 1000\left(\frac{A_{ij}^{*}}{A_{ij}} \cdot \frac{A^{*}}{A}\right)$$

where: W_{ij} has high importance for a certain class i of the parameter j; f_{ij} is the landslide density within class i of parameter j; f is landslide density tho on the whole map; A_{ij}^{*} is a landslide surface in a certain class i of parameter j; A_{ij} is the surface of a certain class i of the parameter j; A* is the total area of the landslide on the entire map; A is the total area of the entire map. In the subsequent step, the weights assigned to each variable are combined in an equation to generate a resultant landslide susceptibility index (LSI) map for the study area. By summing up the weights obtained for each variable, the LSI map provides an integrated representation of landslide susceptibility, incorporating the influence of multiple factors. This map helps identify areas with higher or lower susceptibility to landslides, based on the combined effects of the analyzed variables. The weight values of factors used for the LSA model are presented in Table 5.

Table 5. The weight values of factors used for the LSA model.

Factor	Value	Factor	Value
Lithology		Land coverage	
Clastic sediments	5	Broad-leaved forest	0.5
Tuffs	4	Mixed forest	0.5
Schists	3	Transitional woodland–shrub	2
Dacitic ignimbrites	2	Pastures	4
Andesites	1	Complex cultivation patterns	1
Slopes		Land principally occupied by agriculture	1
0–10°	2	Sparsely vegetated areas	1
10–20°	6	Non-irrigated arable land	1.5
12–30°	10	Urban fabric	1.5
30–40°	8	Bare rocks	4
40–50°	4	Streams	
Convergence (curvature)		0–20 m	2
Concave	5	>20 m	0
Flat	1.5	Roads	
Convex	1.5	0–20 m	2
		>20 m	0

In accordance with [1], a similar approach to the previous method is applied for reclassifying the LSI values into distinct susceptibility zones and performing map validation. The total weighted value assigned to each factor is as follows: 30 for slope, 15 for lithology,

10 for land cover, 8 for curvature, and 2 for stream and road distance, resulting in a cumulative total of 67. These weights indicate the relative importance of each factor in triggering landslides within the catchment. The ratio of these weights is 15:7:5:4:1:1, illustrating that slope is the most influential landslide-causal factor, followed by lithology, land cover, planar curvature, and distance to streams and roads, respectively.

Landslide susceptibility is determined by summing the values of all six parameters. This is performed by aggregating the values for each individual grid cell across all six digital layers. The resulting model is then classified into five distinct classes using natural breaks classification in SAGA GIS 9.0.0 and QGIS 3.30.1-'s-Hertogenbosch software. These classes represent different levels of landslide susceptibility, ranging from very low to very high, as outlined in Table 10. The entire process, including the steps, procedures, and quantitative approaches employed in this study, are summarized in the workflow (Figure 7). Furthermore, each key element of the methodology is described in detail, providing a comprehensive understanding of the study's methodology and analysis.
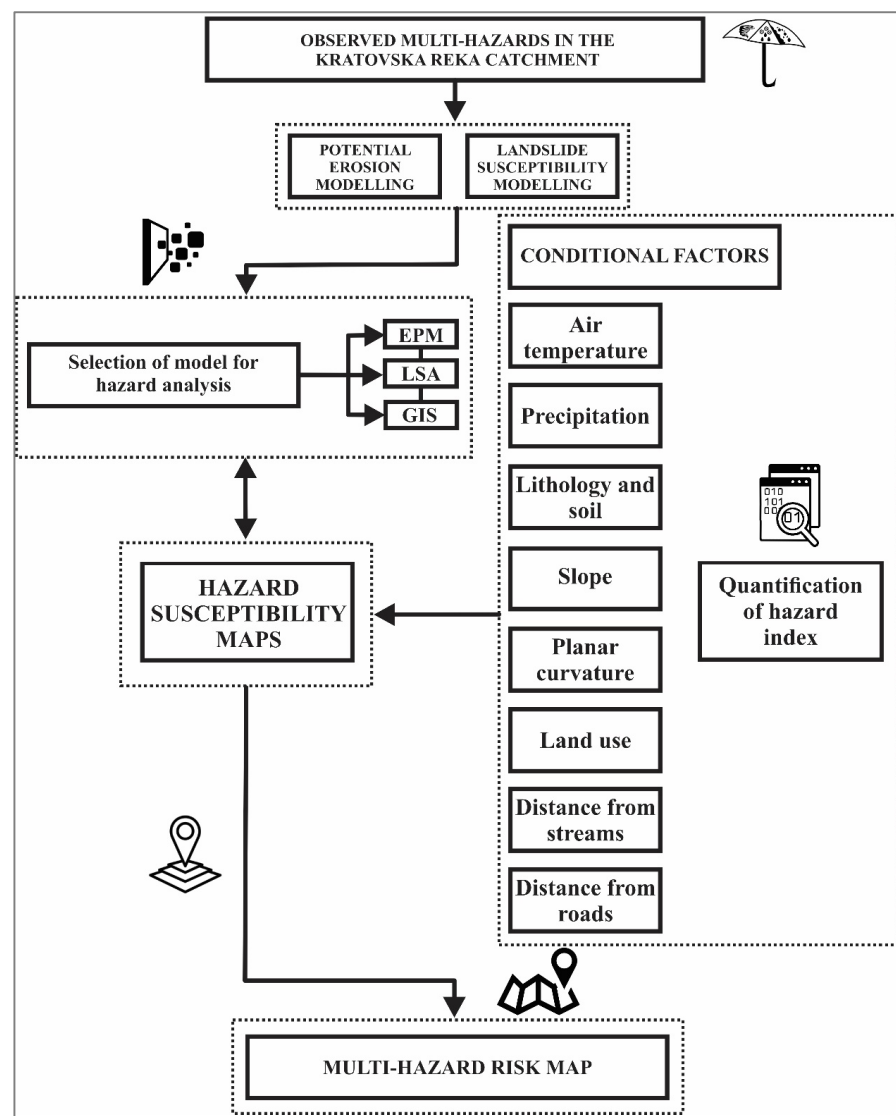

Figure 7. Research workflow.

3. Results

3.1. Erosion Modelling

To calculate the total amount of eroded material, with the help of SAGA GIS, through the previously obtained coefficient of erosion Z (or risk of erosion), an appropriate map was prepared for the Kratovska Reka catchment (Figure 8).
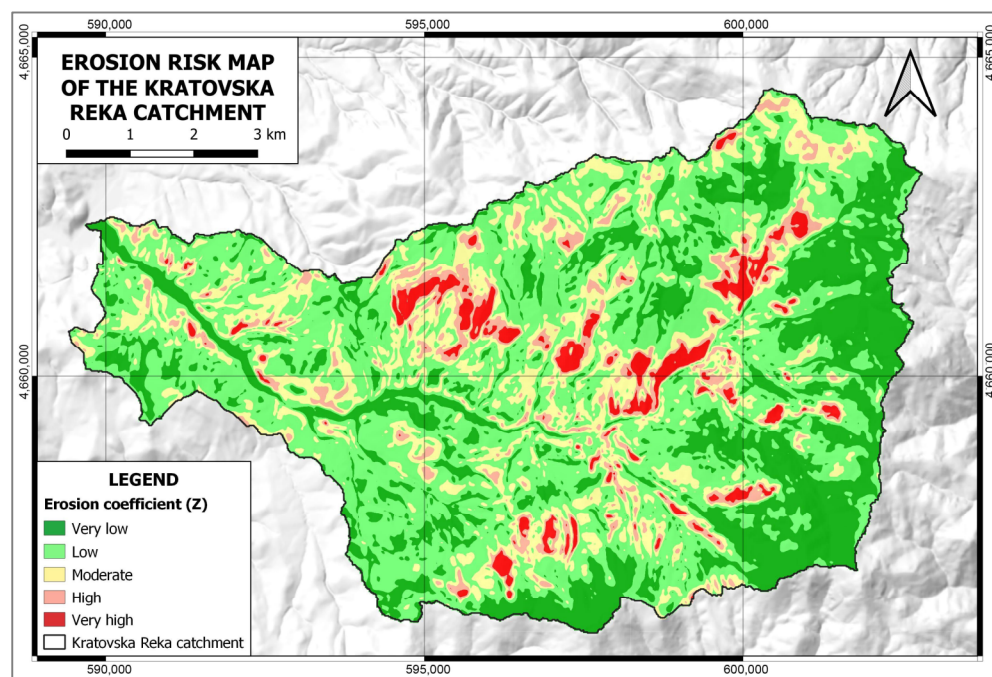

Figure 8. Erosion risk map of the Kratovska Reka catchment (according to Z coefficient values).

The obtained results in the form of the erosion coefficient (Z) show a significant presence of areas with medium, high, and very high risk (values greater than 0.4), which is 28.79 km^2 or almost 50% of the Kratovska Reka catchment (Table 6). These areas experience significant soil erosion and sediment transport, even during moderate rainfall events. The land undergoes strong washing and erosion processes, leading to the production, transportation, and accumulation of deposited material. This behavior is particularly pronounced during intense rainfall with rates exceeding 0.5 mm/min or prolonged periods of heavy rainfall episodes. The eroded material accumulates on the cultivated areas, roads, etc. Otherwise, the mean value of the erosion coefficient Z in the Kratovska Reka catchment is 0.56 (Table 7). Significant factors for such high values of the erosion coefficient are the erodible geological substrate (volcanic tuffs, breccias, slates, Eocene, Miocene, and Pliocene sediments), the bareness–absence of vegetation, and the steep terrain slopes.

Table 6. Areas in the Kratovska Reka catchment subject to the risk of erosion (according to Z coefficient values).

Class	km^2	in %
0–0.4	17.71	25.82
0.4–0.8	31.13	45.39
0.8–1.2	12.91	18.83
1.2–1.6	4.36	6.35
>1.6	2.47	3.61
Total	68.58	100.00

Table 7. Erosion coefficient Z and average annual production of erosive sediment for the Kratovska Reka catchment (P = catchment area; P acc = accumulation area; X*a = coefficient on neatness on the catchment; Koef. Z = coefficient of erosion; W m^3 year = total erosion potential; W m^3/km^2 = specific erosion of a single surface).

Watershed	P km^2	P acc. km^2	X*a	Coef. Z	W m^3/year	W m^3/km^2
Kratovska Reka	68.58	1.16	0.43	0.56	72.709	1063

Based on the findings of the study, it is evident that areas with the highest erosion potential, as indicated by the Z coefficient values, are primarily located along the steep valley sides of the Kratovska Reka and its tributaries. These areas, particularly those lacking adequate vegetation cover or having only sparse grass vegetation, are particularly vulnerable to erosion processes. Due to the absence of protective vegetation, these exposed areas are more susceptible to erosion and the associated risks (Figure 9).

Figure 9. Susceptible areas that are exposed to risks of geohazards of a hydro-meteorological nature (excessive erosion and occurrence of landslides).

The model outputs reveal that the average annual sediment production in the study area amounts to 72.709 m^3, which is a notably high value (Table 7). The most erosive regions within the catchment are identified as the steep valley sides of the Kratovska Reka and its tributaries. These areas, particularly when devoid of vegetation or covered with sparse grassy vegetation, lack protection against the erosive impact of rainfall. Consequently, they are highly susceptible to erosion processes, leading to the substantial sediment production observed in the model results.

Out of the entire watershed area, a significant portion of 17.35% is classified as being at a very high risk of erosion, surpassing 2000 m^3/km^2/year (equivalent to a soil loss of 2 mm per year). This represents a considerable magnitude of erosion. In these high-risk areas, excessive erosion takes place, leading to various erosive landforms, loss of valuable fertile land, and the accumulation of a substantial amount of sediment in riverbeds. Specifically, in the Kratovska Reka valley, there is a distinct belt with significantly high values of specific erosion, ranging from approximately 1500 to 3500 m^3/km^2/year (Table 8). Conversely, in the southeastern, higher parts of the catchment, towards Zletovska Reka, the potential erosion is within normal, natural values below 500 m^3/km^2/year, thanks

to the presence of well-forested areas. To mitigate the degradation and prevent further loss of natural resources, particularly soil and water, it is crucial to implement appropriate preventive conservation measures and activities in areas where the intensity of erosion exceeds 1000 m^3/km^2/year. These measures are essential for preserving the integrity of the ecosystem and safeguarding the valuable resources present in the region.

Table 8. Areas in the Kratovska Reka catchment according to the amount of erosion.

Class	km^2	in %
0–500	16.46	24.01
500–1000	21.39	31.19
1000–1500	11.88	17.33
1500–2000	6.94	10.12
>2000	11.90	17.35
Total	68.58	100.00

In addition to the calculation of eroded material, it is important also to determine the proportion of sediments that reach to the main river (Kriva Reka), as not all sediments exit the Kratovska Reka catchment. Therefore, according to the second part of the EPM approach, the sediment delivery ratio (Ru) is estimated by the following equation

$$Ru = 4(O*D)*0.5/(L + 10)$$

where: O = the length of the catchment border (km), and D = the difference between medium altitude and catchment outlet altitude (km). Specific sediment yield (SSY) is estimated as

$$SSY = W*Ru$$

According to the preceding equation, the average annual transfer of eroded sediment from Kratovska Reka to the estuary of Kriva Reka amounts to 691 m^3/km^2/year (Table 9). This value represents the average quantity of sediment transported from the Kratovska Reka watershed to the downstream area of Kriva Reka on a yearly basis.

Table 9. Average annual transfer (discharge) of eroded sediment from the Kratovska Reka catchment (Hav = mean height of the catchment; Hmin = estuary altitude; O = length of the catchment border (km); Hw = mean height difference of the watershed; L = length of the watershed (km); Ru = retention coefficient; W = average annual sediment production).

Watershed	Hav	Hmin	O	Hw	L	O/L	Ru	W*Ru	Erosion Rate
Kratovska Reka	879	406	42.13	0.473	17.39	2.42	0.65	47.261	691

In addition to identifying potential erosion areas, it is also important to identify areas with high sediment deposition. To accomplish this, we utilized the Topographic Wetness Index (TWI) in SAGA GIS, which effectively highlights valley bottoms. In the case of the Kratovska Reka catchment, the TWI values range from 2.8 to 22.1, with values above 12 being most suitable for determining deposition areas (this was also confirmed through detailed field surveys). By applying this criterion, we calculated an accumulation or deposition area of 1.16 km^2. The majority of the deposition area is located in the Kratovska Reka valley, specifically downstream of the town of Kratovo (see Figure 10). The significant portion of eroded material, which amounts to an average of 25,448 m^3/year, is primarily accumulated within this deposition area, particularly during flood events, on top of the fluvisols. The sediment carried by these floods consists of a variety of particle sizes, ranging from pebbles and gravel to sand, silt, and clay (mud), thus leading to alterations in the soil structure. The distribution of sediment types on the floodplain is determined by the energy of the water flow. In close proximity to the river, only the larger-sized material, such as

sand, can deposit, due to the strong current. In areas where the flow is relatively lower, silt and fine sand tend to deposit predominantly.
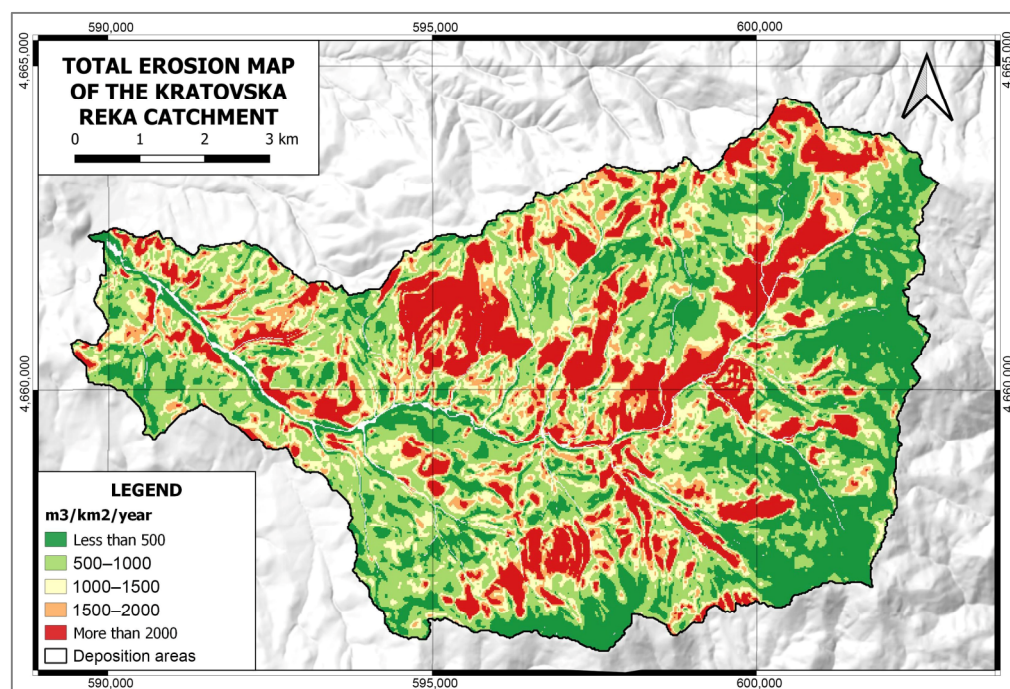

Figure 10. Total erosion map of the Kratovska Reka catchment.

3.2. Landslide Susceptibility Modelling

According to the probability map of the occurrence of landslides in the Kratovska Reka catchment, created with the help of the LSI + AHP natural breaks classification and the prepared Table 10, we can determine that class 3 is represented at the highest level (33.17%), with an average probability of occurrence of landslides, on the steep valley sides of the Kratovska Reka and the source parts of its left and valley sides of the right tributaries (Figure 11).

Table 10. Landslide susceptibility areas in the Kratovska Reka catchment according to the natural breaks classification.

Class	km^2	%
1	1.05	1.53
2	7.86	11.47
3	22.75	33.17
4	14.28	20.82
5	22.65	33.03
Total	68.58	100.00

Subsequently, the second and a similar percentage representation (33.03%) is recorded by class 5, with a very high (also the highest) probability of landslides, and with the greatest intensity in the valley of the Kratovska Reka, downstream of the town of Kratovo, and the valleys of the left tributaries. With 20.82%, class 4 is represented, with a high intensity of occurrence of landslides, with the highest representation along the valley and source sides of the right tributaries of the Kratovska Reka, as well as in the lower (western) part of the catchment area, more precisely, downstream at the confluence in Kriva Reka. Class 2, with low intensity of probability of occurrence of landslides, is represented (11.47%) in a very small area, specifically in the catchment of the left tributary of the Kratovska Reka, Latišnica, and around the volcanic mounds in the southern part of the catchment. The

first susceptibility class (class 1), representing the smallest and nearly negligible portion (1.53%) of the total probability, corresponds to areas with a very low intensity of landslide occurrence. These areas are predominantly located on the volcanic mounds in the southern part of the study area. The low probability of landslides in this class suggests that these areas are relatively stable and less prone to landslide events, compared to other parts of the region.
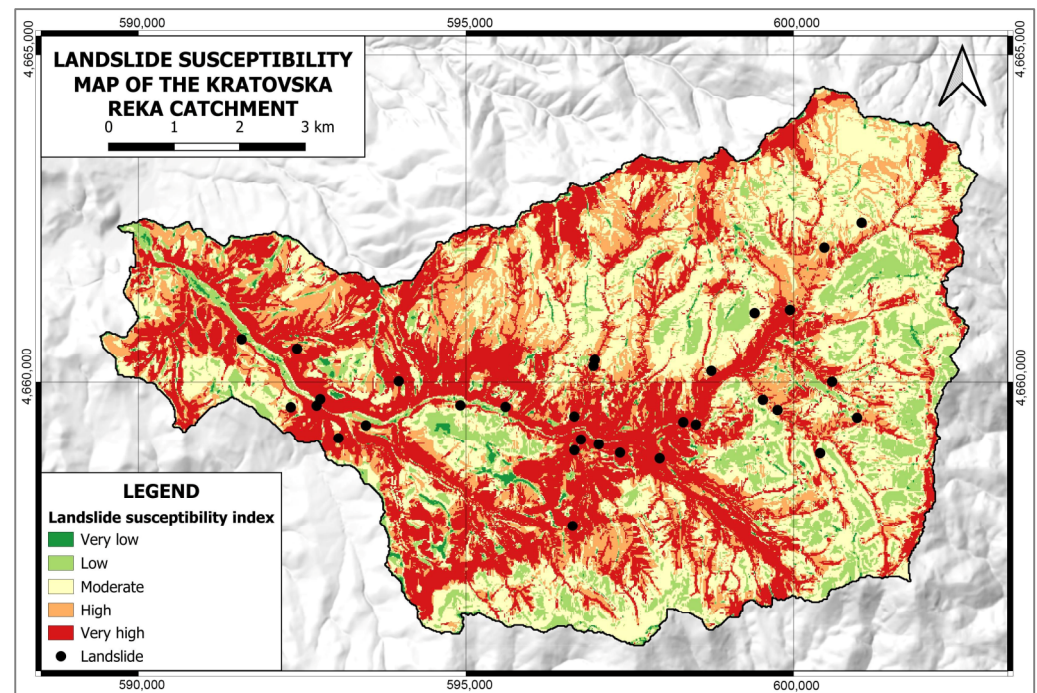

Figure 11. Landslide susceptibility map of the Kratovska Reka catchment according to the natural breaks classification (m^3/km^2 year).

A crucial step in LSA is model validation. To achieve this, a comparison was made between the locations of landslides recorded during a field trip (a total of 31) and the LSA zonation. The results of this comparison are defined in Table 11.

Table 11. Location of the recorded landslides in relation to the LSI classes.

Class	No	%
1	0	0.0
2	1	3.2
3	5	16.1
4	6	19.4
5	19	61.3
Total	31	100.0

Thus, out of the total of 31 landslides, 19 (or 61.3%) are located in the very high LSI zone. When combined with the high LSI zone (class 4), the overlap accounts for 80.7% of the recorded landslides, indicating a very high level of accuracy for the implemented model.

In order to assess the overall performance of the LSA model for the study area, additional validation analysis was conducted using the receiver operating characteristics (ROC) curve and the area under the curve (AUC) value [43]. The AUC value characterizes the quality of the probabilistic model by indicating its reliability in predicting the occurrence or non-occurrence of events. A good fit is represented by AUC values ranging from 0.5 to 1, while values below 0.5 indicate a random fit [100]. For a more comprehensive evaluation of the model, in addition to the 31 recorded true-positive landslides (with a value of 1) in

the validation dataset, a number of false-positive landslides (with a value of 0) were also selected. It is generally recommended to have 2–3 times more false-positive landslides than true landslides for proper validation [101]. In our case, 90 false-positive landslides were randomly selected as sampling points from the digital elevation model (DEM) using SAGA GIS, followed by careful inspection. It is important to note that the selection of false-positive landslides (0) should be performed cautiously to avoid inadequate or confusing results [54].

The ROC curve and AUC value in this study were calculated using SPSS statistical software and are presented in Figure 12. Based on the calculated data, the AUC value is determined to be 0.856, indicating a good level of accuracy for the model employed.
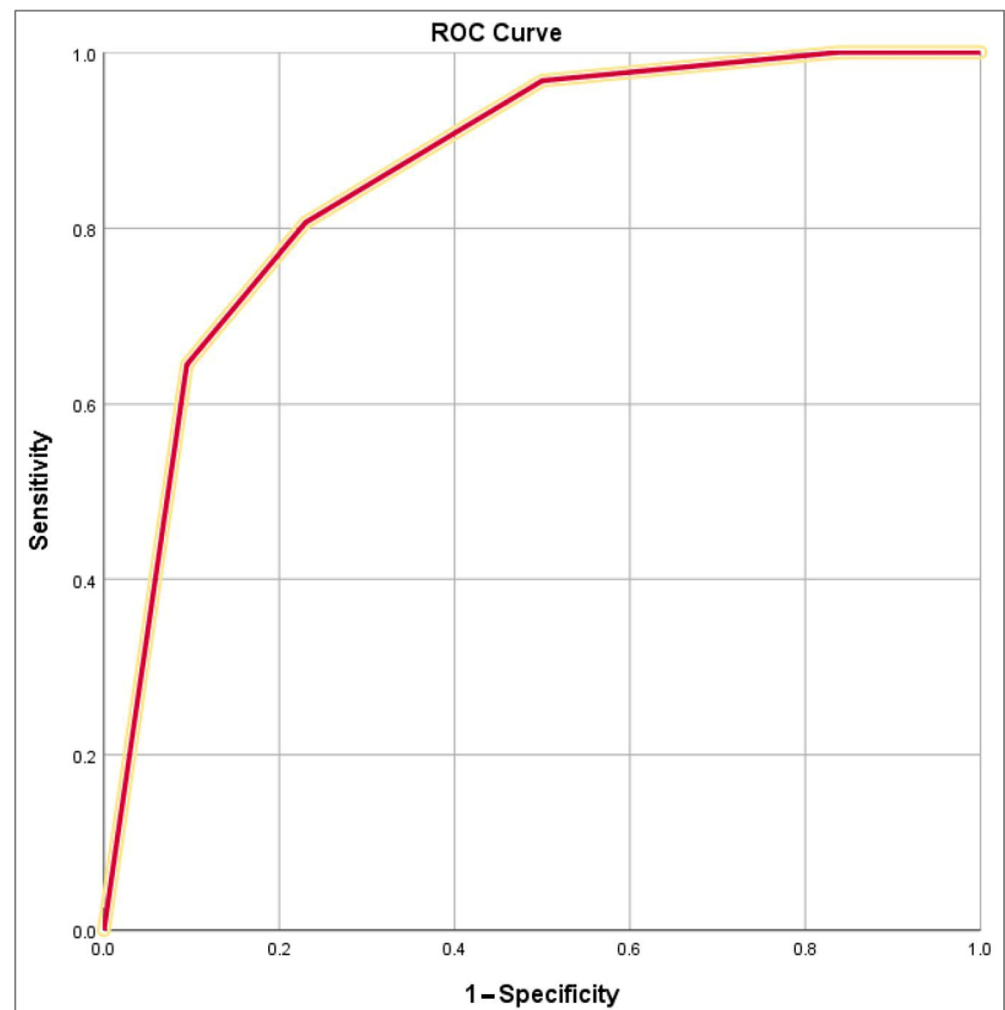

Figure 12. ROC curve and AUC value for the LSI model of the Kratovska Reka catchment.

3.3. Multi-Hazard (Combined Erosion and Landslides) Modelling

According to the study's objective, a geohazard map was prepared by combining erosion and landslide susceptibility maps (Figure 13). Using SAGA GIS software, the areas with high erosion potential were overlapped with the areas highly susceptible to landslides. In this way, the areas heavily endangered by both hazards (multi-hazard) are identified.

The analysis conducted using a special procedure in SAGA GIS reveals that a portion of the Kratovska Reka catchment is at risk from multiple hazards, namely landslides and excessive erosion. This area, referred to as the "total at risk" in the study, encompasses approximately 3.13% of the total catchment area (Table 12). These multi-hazard zones are predominantly located along the valley sides of Kratovska (Tabačka) Reka, extending from the village of Gorno Kratovo, downstream to the city of Kratovo. The terrain in this area is characterized by deforestation, bare ground, steep slopes, and the presence of

weakly resistant rocks. It is important to note that there is also a potential danger to the surrounding houses situated in these high-risk zones.
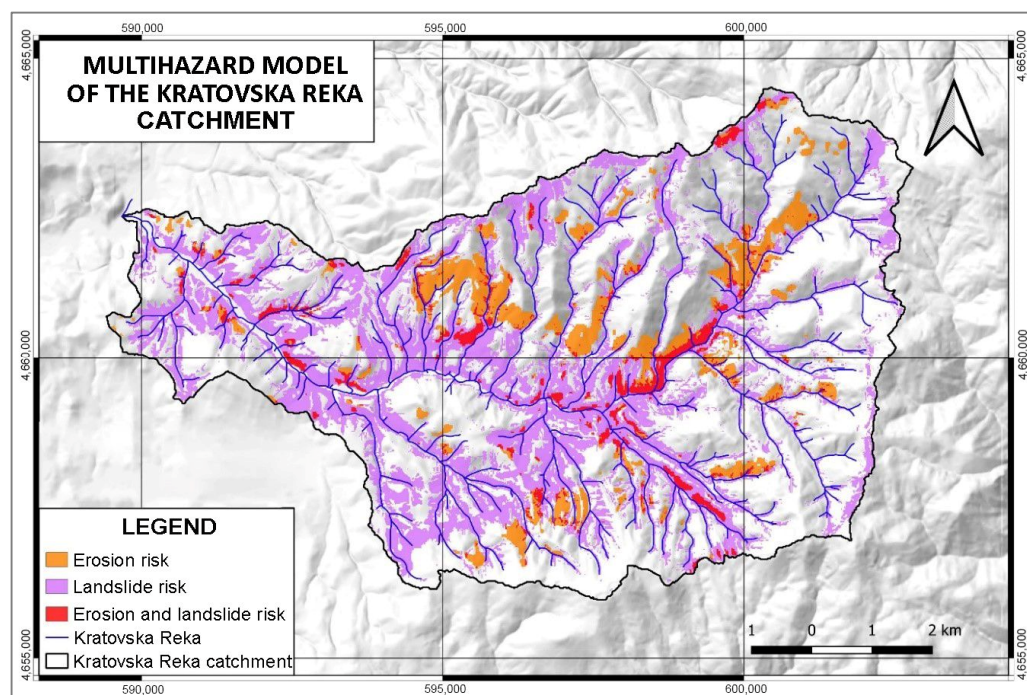

Figure 13. Multi-hazard map of the Kratovska Reka catchment.

Table 12. Areas with a high risk of erosion, landslides, and multi-hazard in the Kratovska Reka catchment.

Geohazards	Area	
	km^2	%
Landslides	22.65	33.03
Excessive erosion	6.83	9.96
Multi-hazard	2.15	3.13
Total at risk	27.33	39.86
Total	68.58	100

4. Discussion

Soil degradation has a significant impact on soil productivity, leading to reduced agricultural yields and ecosystem functionality [44]. To effectively manage soil erosion and assist decision-makers in implementing appropriate remediation measures and mitigation strategies, it is crucial to monitor and assess the system to gather accurate and reliable information on soil erosion under current climate and land use conditions [102]. This information serves as a foundation for understanding the extent of soil degradation and identifying areas that require intervention to prevent further erosion and restore soil health. By obtaining comprehensive data on soil erosion dynamics, policymakers and land managers can make informed decisions and develop targeted strategies for sustainable land management practices.

According to the obtained results of the EPM, it follows that Kratovska Reka has an erosive catchment area. The slope of the initial relief has the biggest impact on the Kratovska Reka catchment and the fluvial processes in it. The annual transfer of eroded sediment from Kratovska Reka to the estuary in Kriva Reka averages 691 m^3/km^2/year. The average annual sediment production is 72.709 m^3. The values of the erosion coefficient (Z) show a significant presence of terrains with medium, high, and very high risk (values greater

than 0.4), which comprises 28.79 km^2 or almost 50% of the Kratovska Reka catchment. Otherwise, the average value of the erosion coefficient Z in the catchment is 0.56. Of the total area of the Kratovska Reka catchment, as much as 17.35% is under a very high risk of erosion, which exceeds 2000 m^3/km^2/year (a soil layer of 2 mm per year), which is a huge value. Excessive water erosion occurs here, which causes the creation of numerous erosive relief phenomena, the loss of fertile areas, and the filling of riverbeds with a large amount of sedimentary material. The specific erosion rate in the Kratovska Reka catchment is estimated to be 1286.5 m^3/km^2/year. The high specific erosion rate suggests that the investigated catchment experiences significant erosion rates, leading to the loss of soil and sediment deposition in the river system.

In comparison to the entire Kriva Reka catchment, the Kratovska Reka catchment exhibits higher erosivity, with a coefficient Z of 0.56 compared to 0.51. Additionally, the average annual erosion rate for the Kratovska Reka catchment is estimated to be 1063 m^3/km^2/year, whereas the Kriva Reka catchment has an erosion rate of 805 m^3/km^2/year. These results indicate that the average annual erosion in the Kratovska Reka catchment is nearly twice as high as the average specific erosion rate for the entire territory of North Macedonia, which is reported as 681 m^3/km^2/year according to [50]. Furthermore, a comparison was made with a similar-sized study area, the municipality of Štrpce in southern Serbia. In a study [103], it was found that 55.20% of the Kratovska Reka catchment exhibits low erosion rates, whereas the majority of the Štrpce municipality (50.03%) displays low erosion rates. Similar observations have been made by studies conducted by [38,45,104], which indicate that the intensity of soil erosion is closely linked to dynamic interactions among natural conditions, demographic and settlement indicators, and changes in land use.

This study considered six factors as preconditions for landslide occurrence, namely slope, lithology, land cover, plan curvature, distance from streams, and distance from roads. These factors were converted into raster format and standardized to a cell size of 15 m × 15 m. The results revealed that a significant portion of the catchment (1/3) falls into the class with a very high probability of landslides, particularly in the downstream valley of the Kratovska Reka, below the city of Kratovo, and in the valleys of its left tributaries. The analysis also identified the steep valley sides of Kratovska Reka and the upper reaches of its right tributaries as areas with the highest probability of landslide occurrence. Conversely, the higher mountainous regions, characterized by lower slopes and composed of solid and compact volcanic rocks, exhibit a lower probability of landslides. Overall, the high-risk class, indicating a significant likelihood of landslides, encompasses approximately 33.03% of the Kratovska Reka catchment.

At the national level, the regions in North Macedonia with high and very high landslide susceptibility are predominantly found in hilly terrain, mountain foothills, valley bottoms, gorges, depressions, and basins [54]. These areas are typically characterized by the presence of Neogene lacustrine sediments. In terms of the entire country, a significant portion (18.9% according to the LSI model, 33.4% according to the LSI + AHP model, and 40.1% according to the AHP model) falls into high and very high landslide susceptibility zones, as verified by the landslide dataset [54]. In comparison, the Kratovska Reka catchment exhibits a higher susceptibility to landslides, when compared to the findings of [54]. Results provided by this study indicate that the Kratovska Reka catchment is particularly prone to landslides, highlighting the need for appropriate measures and strategies to mitigate the associated risks in the area.

In order to enhance the mitigation measures and approaches, several aspects should be taken into consideration. Firstly, there should be a significant improvement in the inventory of landslide data, ensuring its accuracy and completeness. Additionally, the spatial resolution of the precondition data layers should be enhanced to capture more detailed information. Improving the weighting of factors is another important aspect, as it can contribute to a more accurate assessment of landslide susceptibility. This may involve refining the weights assigned to different factors based on their relative importance and influence on landslide occurrence. Furthermore, the inclusion of additional precondition

factors can enhance the model's predictive capabilities. Factors such as the topographic wetness index (TWI), stream power index (SPI), normal difference vegetation index (NDVI), geological structural elements, precipitation intensities, and other indicators can provide valuable insights into the susceptibility of an area to landslides (mass movements-wet).

Moreover, it is recommended that alternative model validation approaches, such as those proposed by [105–107], are explored. This can help ensure the robustness and reliability of the susceptibility models. Overall, a comprehensive assessment of total susceptibility to natural hazards can provide valuable information for identifying vulnerable areas and implementing measures to protect the environment, as well as natural and cultural heritage [79,108–110].

The terrain characteristics of the Kratovska Reka catchment in North Macedonia, including steep slopes and surface disintegration of rocks, make it susceptible to various geohazards (see Figure 13). Among these hazards, excessive water erosion and landslides are particularly prominent. To assess and understand these risks, accurate GIS-based models have been developed to determine the potential occurrence of such hazards. These models indicate that a significant portion of the Kratovo municipality within the catchment area is at risk of experiencing these hazards in the upcoming multi-year period. The results hold significant importance for the local community and various institutions involved in environmental protection and emergency management. By providing an overview of the most potentially endangered locations in the area, these results serve as a valuable resource for decision-making and planning purposes [103]. They help stakeholders identify areas that require special attention and prioritize efforts to mitigate risks, protect communities, and manage emergencies effectively.

The places with the highest erosion potential and the riskiest parts for the probability of landslides are on the steep valley sides of the Kratovska Reka and its tributaries, and the source parts of the right tributaries, especially in places that are completely exposed or are under sparse grassy vegetation and unprotected from the erosive effect of rain. Precisely because of the above, the bare and steep valley sides of the Kratovska Reka and its tributaries, with an excessive amount of precipitation, can contribute to an increase in the intensity of erosion and the occurrence of landslides.

Within the Kratovska Reka catchment area, 3.13% of the total area is categorized as multi-hazard zones, meaning they are prone to both landslides and excessive water erosion. These areas are primarily located along the valley sides of the Kratovska (Tabačka) Reka, spanning from the village of Gorno Kratovo, downstream to the town of Kratovo. The terrain in these zones is characterized by deforestation, lack of vegetation cover, steep slopes, and the presence of rocks with low resistance to erosion. These factors contribute to the heightened vulnerability of these areas to multiple geohazards.

In the Kratovska Reka catchment, it is crucial to comprehensively assess the erosion situation, both remotely and in the field, in order to define and implement appropriate anti-erosion measures to mitigate the intensity of erosion and soil loss. It is important to prioritize the dominant hazards, in order to implement targeted preventive measures. Considering the specific conditions and physical characteristics of the investigated area, measures can be tailored to address the most significant hazards, such as landslides and excessive water erosion. By focusing on these dominant hazards, it is possible to develop and implement effective preventive strategies that mitigate the risks associated with soil loss and protect the environment, natural resources, and infrastructure in the catchment.

The standardization and implementation of multi-hazard methodologies would be a significant step towards enhancing the qualitative monitoring and identification of geohazards at the local and regional scale in North Macedonia. This approach would emphasize the importance of risk assessment and management programs, which are currently under development in this part of southeast Europe. Furthermore, future studies could expand on this work by conducting broader research that covers the entire territory of North Macedonia.

The maps and calculations derived from this research could serve as a foundation for a comprehensive inventory of hydro-meteorological hazardous events. Such an inventory would provide valuable knowledge for establishing appropriate management and mitigation guidelines and measures, not only within the studied area but also at regional and national levels in the region [38]. This would greatly contribute to improving the overall understanding and response to geohazards in North Macedonia, leading to more effective risk management and enhanced resilience to natural disasters induced by climate change.

The research included a crucial aspect of validating the results obtained from the implemented approach. The most effective validation tool for the erosion potential model (EPM) is comparing the model results with the average annual sedimentation in reservoirs that rivers flow into, typically measured using echo sonars. Unfortunately, there are no such reservoirs in the Kratovska Reka catchment or its larger recipient, the main river of Kriva Reka. Another option for future investigations is comparing the model results with measured sediment load, but the only gauge station nearby is located on the main river, Kriva Reka, near the village of Trnovac. However, a similar GIS-based EPM approach implemented by [50] on the Kriva Reka has demonstrated that the model produces highly accurate results when comparing sediment transport through the river profile. To further enhance the accuracy of the model, the installation of a gauge station with sediment transport measurements near the outlet of Kratovska Reka would provide a direct opportunity for result comparison and validation. Until then, it is considered that the model's comparison with sedimentation data for the entire Kriva Reka catchment, as well as the heuristic approach involving opinions from three additional national erosion experts regarding soil erosion quantity based on the national maps, demonstrates acceptable accuracy of the obtained results.

Validating the landslide susceptibility model is relatively easier, as it requires at least a basic landslide inventory. In this regard, the positions of the 31 landslides recorded during the field survey were compared with the model's zonation, resulting in an 80.7% overlap with the high and very high susceptibility zones.

The ROC curve and AUC value in this study were also calculated. Based on the calculated data, the AUC value was determined to be 0.856, indicating a good level of accuracy for the model employed. Additional validation can be conducted by analyzing the Kappa values. Furthermore, it is crucial to emphasize the necessity for further research, particularly related to the validation of results using precise LIDAR measurements and other advanced technologies to assess whether erosion and landslide risks are increasing or decreasing in this part of North Macedonia.

5. Conclusions

The analysis of territories that are highly susceptible to geohazards plays a crucial role in facilitating the adoption of appropriate preventive measures and effective environmental management actions by local, provincial, and state services [103]. The primary objective of a multi-hazard map is to identify and delineate hazardous areas, thereby aiding in activities aimed at reducing the hazards and mitigating future damage [55,56]. This becomes particularly significant when considering the impact of climate change, which is associated with increased landslide activity and excessive erosion. The approach presented in the paper has the potential to generate reliable multi-hazard maps at the national level and provide valuable information for regional planning and decision-making processes. By utilizing such maps, stakeholders can make informed choices and take appropriate measures to minimize the risks associated with geohazards and enhance overall resilience to environmental challenges.

The Kratovska Reka catchment, with its distinctive physical characteristics, geographical position, and rich geodiversity, offers an ideal setting for conducting a comprehensive analysis of geohazards on a regional basis. Utilizing Geographic Information Systems (GIS), relevant data pertaining to the entire research area were used to analyze and assess the extent of excessive and water erosion, susceptibility to landslides, and identify areas

prone to multi-hazards. By leveraging the capabilities of GIS, a holistic understanding of the interaction between the geohazard and landscape within the case study was achieved. Creating a cadastre of areas endangered by geohazards in the Kratovska Reka catchment can indeed be a valuable future goal. Such a cadastre could serve as an essential tool for sustainable spatial and urban planning, thus enabling decision-makers to incorporate hazard mitigation measures into development plans, in order to reduce unfavorable effects on natural resources, the local economy, and socio-demographic processes.

Landslides have been identified as the predominant geohazard in the Kratovska Reka catchment, accounting for approximately 33.03% of the total area vulnerability. Additionally, the analysis of excessive erosion revealed a mean erosion coefficient of 0.56, indicating a high level of erosion within the analyzed catchment. Nearly 50% of the area is affected by the highlighted erosion processes. By integrating the analysis of these two geohazards using GIS techniques and employing methods such as natural breaks, a multi-hazard model combining water erosion and mass movements (wet) was derived for regional scale analysis. This model indicates that 3.13% of the catchment is highly or very highly susceptible to the combined effects of water erosion and landslides. The overall risk associated with these geohazards, including the multi-hazard susceptibility, amounts to 39.86% of the catchment area. These findings emphasize the importance of addressing both landslides and excessive erosion in the management and mitigation of geohazards within the Kratovska Reka catchment in North Macedonia.

In this area, which is a part of the Kratovo-Zletovo paleovolcanic area, combining the obtained results with field research is crucial for effectively preserving and protecting the geodiversity values. The results of this work contribute to the growing evidence of erosion risk in southeast Europe [22], shedding light on the specific challenges and vulnerabilities within the Kratovska Reka catchment in North Macedonia. The identification and assessment of erosion risk in this part of the region provide valuable information for understanding the broader patterns and dynamics of erosion processes in southeast Europe [25–27]. The findings can be used as a foundation for further research and refinements in erosion risk assessment methodologies, including the incorporation of additional factors, validation techniques, and improved modelling approaches [55–60].

References

1. Milevski, I.; Dragićević, S. GIS-Based Landslide Susceptibility Modelling of the Territory of the Republic of Macedonia. In Proceedings of the 7th International Conference on Cartography and GIS, Sozopol, Bulgaria, 18–23 June 2018; pp. 82–91.
2. Salvati, P.; Petrucci, O.; Rossi, M.; Bianchi, C.; Pasqua, A.A.; Guzzetti, F. Gender, Age and Circumstances Analysis of Flood and Landslide Fatalities in Italy. *Sci. Total Environ.* **2018**, *610–611*, 867–879. [CrossRef] [PubMed]
3. Alam, E.; Ray-Bennett, N.S. Disaster Risk Governance for District-Level Landslide Risk Management in Bangladesh. *Int. J. Disaster Risk Reduct.* **2021**, *59*, 102220. [CrossRef]
4. Li, X.; Huang, X.; Zhang, Y. Spatio-temporal Analysis of Groundwater Chemistry, Quality and Potential Human Health Risks in the Pinggu Basin of North China Plain: Evidence from High-Resolution Monitoring Dataset of 2015–2017. *Sci. Total Environ.* **2021**, *800*, 149568. [CrossRef] [PubMed]
5. Shinohara, Y.; Kume, T. Changes in the Factors Contributing to the Reduction of Landslide Fatalities between 1945 and 2019 in Japan. *Sci. Total Environ.* **2022**, *827*, 154392. [CrossRef] [PubMed]
6. Rosenbaum, M.S.; Culshaw, M.G. Communicating the Risks Arising from Geohazards. *J. R. Stat. Soc. A* **2003**, *166*, 261–270. [CrossRef]
7. Yang, H.-Q.; Zhang, L.; Gao, L.; Phoon, K.-K.; Wei, X. On the Importance of Landslide Management: Insights from a 32-year Database of Landslide Consequences and Rainfall in Hong Kong. *Eng. Geol.* **2022**, *299*, 106578. [CrossRef]
8. Mertens, K.; Jacobs, L.; Maes, J.; Kabaseke, C.; Maertens, M.; Poesen, J.; Kervyn, M.; Vranken, L. The Direct Impact of Landslides on Household Income in Tropical Regions: A Case Study from the Rwenzori Mountains in Uganda. *Sci. Total Environ.* **2016**, *550*, 1032–1043. [CrossRef]
9. Pham, N.T.T.; Nong, D.; Garschagen, M. Natural Hazard's Effect and Farmers' Perception: Perspectives from Flash Floods and Landslides in Remotely Mountainous Regions of Vietnam. *Sci. Total Environ.* **2020**, *759*, 142656. [CrossRef]
10. Moniruzzaman, S. Income and Consumption Dynamics after Cyclone Aila: How Do the Rural Households Recover in Bangladesh? *Int. J. Disaster Risk Reduct.* **2019**, *39*, 101142. [CrossRef]
11. Yao, D.; Xu, Y.; Zhang, P. How a Disaster Affects Household Saving: Evidence from China's 2008 Wenchuan Earthquake. *J. Asian Econ.* **2019**, *64*, 101133. [CrossRef]
12. Sapkota, J.B. Human Well-Being after 2015 Nepal Earthquake: Micro-evidence from One of the Hardest Hit Rural Villages. *Int. J. Sustain. Dev.* **2018**, *21*, 54–74. [CrossRef]
13. Berlemann, M.; Eurich, M. Natural Hazard Risk and Life Satisfaction-Empirical Evidence for Hurricanes. *Ecol. Econ.* **2021**, *190*, 107194. [CrossRef]
14. Burrows, K.; Desai, M.U.; Pelupessy, D.C.; Bell, M.L. Mental Well-being Following Landslides and Residential Displacement in Indonesia. *SSM-Ment. Health* **2021**, *1*, 100016. [CrossRef]
15. Vereb, V. Geoheritage and Resilience. Selected Studies of Volcanic Geo-Heritage Areas from Different Geographical Environments and Different Levels of Protection. Ph.D. Thesis, Doctoral School of Earth Sciences, Eötvös Loránd University, Budapest, Hungary, 2020.
16. Coratza, P.; De Waele, J. Geomorphosites and Natural Hazards: Teaching the Importance of Geomorphology in Society. *Geoheritage* **2012**, *4*, 195–203. [CrossRef]
17. Milevski, I. The Biggest Natural Hazards in Macedonia in the Last 100 Years. IGEO Portal. Available online: igeoportal.net/?p=6863 (accessed on 28 September 2016). (In Macedonian)
18. Lukić, T.; Gavrilov, M.B.; Marković, S.B.; Komac, B.; Zorn, M.; Mladjan, D.; Đorđević, J.; Milanović, M.; Vasiljević, Đ.A.; Vujičić, M.D.; et al. Classification of the natural disasters between the legislation and application: Experience of the Republic of Serbia. *Acta Geogr. Slov.* **2013**, *53*, 149–164. [CrossRef]
19. Turconi, L.; Faccini, F.; Marchese, A.; Paliaga, G.; Casazza, M.; Vojinovic, Z.; Luino, F. Implementation of Nature-Based Solutions for Hydro-Meteorological Risk Reduction in Small Mediterranean Catchments: The Case of Portofino Natural Regional Park, Italy. *Sustainability* **2020**, *12*, 1240. [CrossRef]
20. Valjarević, A.; Filipović, D.; Valjarević, D.; Milanović, M.; Milošević, S.; Živić, N.; Lukić, T. GIS and remote sensing techniques for the estimation of dew volume in the Republic of Serbia. *Meteorol. Appl.* **2020**, *27*, 1930. [CrossRef]
21. Ivkov, M.; Blešić, I.; Janićević, S.; Kovačić, S.; Miljković, Đ.; Lukić, T.; Sakulski, D. Natural Disasters vs Hotel Industry Resilience: An Exploratory Study among Hotel Managers from Europe. *Open Geosci.* **2019**, *11*, 378–390. [CrossRef]
22. Rüttinger, L.; van Ackern, P.; Gordon, N.; Adrian, F. *Regional Assessment for South-Eastern Europe: Security Implications of Climate Change*; OSCE: Adelphi, MD, USA; Berlin, Germany, 2021; pp. 1–73.
23. United Nations Office for Disaster Risk Reduction. Available online: www.unisdr.org/files/1741_SouthEasternEuropeDRMitigation.pdf (accessed on 25 August 2022).
24. Kurnik, B.; van der Linden, P.; Mysiak, J.; Swart, R.J.; Füssel, H.M.; Christiansen, T.; Cavicchia, L.; Gualdi, S.; Mercogliano, P.; Rianna, G.; et al. *Climate Change Adaptation and Disaster Risk Reduction in Europe: Enhancing Coherence of the Knowledge Base, Policies and Practices*; EEA-European Environment Agency: Copenhagen, Denmark, 2017; pp. 1–176.
25. Spinoni, J.; Vogt, J.V.; Naumann, G.; Barbosa, P.; Dosio, A. Will drought events become more frequent and severe in Europe? *Int. J. Climatol.* **2018**, *38*, 1718–1736. [CrossRef]

26. Insana, A.; Beroya-Eitner, M.A.; Barla, M.; Zachert, H.; Žlender, B.; van Marle, M.; Kalsnes, B.; Bračko, T.; Pereira, C.; Prodan, I.; et al. Climate Change Adaptation of Geo-Structures in Europe: Emerging Issues and Future Steps. *Geosciences* **2021**, *11*, 488. [CrossRef]

27. Cvetković, V.M.; Grbić, L. Public perception of climate change and its impact on natural disasters. *J. Geogr. Inst. Jovan Cvijic SASA* **2021**, *71*, 43–58. [CrossRef]

28. Blešić, I.; Ivkov, M.; Tepavčević, J.; Popov Raljić, J.; Petrović, M.D.; Gajić, T.; Tretiakova, T.N.; Syromiatnikova, J.A.; Demirović Bajrami, D.; Aleksić, M.; et al. Risky Travel? Subjective vs. Objective Perceived Risks in Travel Behaviour—Influence of Hydro-Meteorological Hazards in South-Eastern Europe on Serbian Tourists. *Atmosphere* **2022**, *13*, 1671. [CrossRef]

29. Güneralp, B.; Güneralp, I.; Liu, Y. Changing global patterns of urban exposure to flood and drought hazards. *Glob. Environ. Chang.* **2015**, *31*, 217–225. [CrossRef]

30. Pörtner, H.-O.; Roberts, D.C.; Tignor, M.; Poloczanska, E.S.; Mintenbeck, K.; Alegría, A.; Craig, M.; Langsdorf, S.; Löschke, S.; Möller, V.; et al. (Eds.) Climate Change 2022: Impacts, Adaptation and Vulnerability. In *Contribution of Working Group II to the Sixth Assessment Report of the Intergovernmental Panel on Climate Change*; Cambridge University Press: Cambridge, UK; New York, NY, USA, 2022; p. 3056.

31. Dilley, M.; Chen, R.S.; Deichmann, M.; Lerner-Lam, A.; Arnold, M.; Agwe, J.; Buys, P.; Kjekstad, O.; Lyon, B.; Yetman, G. *Natural Disaster Hotspots: A Global Risk Analysis*; World Bank Publications: Washington, DC, USA, 2005.

32. Gaume, E.; Borga, M. Post-flood field investigations in upland catchments after major flash floods: Proposal of a methodology and illustrations. *J. Flood Risk Manag.* **2008**, *1*, 175–189. [CrossRef]

33. Smith, K.; Petley, D.N. Environmental Hazards. In *Assessing Risk and Reducing Disaster*, 5th ed.; Routledge: London, UK; New York, NY, USA, 2009; p. 383.

34. Marchi, L.; Borga, M.; Preciso, E.; Gaume, E. Characterization of selected extreme flash floods in Europe and implications for flood risk management. *J. Hydrol.* **2010**, *394*, 118–133. [CrossRef]

35. Gencer, E.A. Natural Disasters, Urban Vulnerability, and Risk Management: A Theoretical Overview. In *The Interplay between Urban Development, Vulnerability, and Risk Management, Mediterranean Studies*; Gencer, E.A., Ed.; Springer: Berlin/Heidelberg, Germany, 2013; Volume 7, Chapter 2; pp. 7–43.

36. Arnell, N.; Gosling, S. The impacts of climate change on river flow regimes at the global scale. *J. Hydrol.* **2013**, *486*, 351–364. [CrossRef]

37. Hirabayashi, Y.; Mahendran, R.; Koirala, S.; Konoshima, L.; Yamazaki, D.; Watanabe, S.; Kim, H.; Kanae, S. Global flood risk under climate change. *Nat. Clim. Chang.* **2013**, *3*, 816–821. [CrossRef]

38. Ristanović, B.; Cimbaljević, M.; Miljković, Đ.; Ostojić, M.; Fekete, R. GIS Application for Determining Geographical Factors on Intensity of Erosion in Serbian River Basins. Case Study: The River Basin of Likodra. *Atmosphere* **2019**, *10*, 526. [CrossRef]

39. Ighodaro, I.D.; Lategan, F.S.; Yusuf, S.F.G. The impact of soil erosion on agricultural potential and performance of Sheshegu community farmers in the Eastern Cape of South Africa. *J. Agric. Sci.* **2013**, *5*, 140–147. [CrossRef]

40. Durlević, U.; Momčilović, A.; Ćurić, V.; Dragojević, M. Gis application in the analysis of erosion intensity in the Vlasina River Basin. *Bull. Serbian Geogr. Soc.* **2019**, *99*, 17–36. [CrossRef]

41. Stefanidis, S.; Chatzichristaki, C.; Stefanidis, P. An ArcGIS toolbox for estimation and mapping soil erosion. *J. Environ. Prot. Ecol.* **2021**, *22*, 689–696.

42. Micić Ponjiger, T.; Lukić, T.; Wilby, R.L.; Marković, S.B.; Valjarević, A.; Dragićević, S.; Gavrilov, M.B.; Ponjiger, I.; Durlević, U.; Milanović, M.M.; et al. Evaluation of Rainfall Erosivity in the Western Balkans by Mapping and Clustering ERA5 Reanalysis Data. *Atmosphere* **2023**, *14*, 104. [CrossRef]

43. Fawcett, T. An introduction to ROC analysis. *Pattern Recognit. Lett.* **2006**, *27*, 861–874. [CrossRef]

44. Gocić, M.; Dragićević, S.; Radivojević, R.; Martić Bursać, N.; Stričević, L.; Đorđević, M. Changes in soil erosion intensity caused by land use and demographic changes in the Jablanica River Basin, Serbia. *Agriculture* **2020**, *10*, 345. [CrossRef]

45. Gocić, M.; Dragićević, S.; Živanović, S.; Ivanović, R.; Martić Bursać, N.; Stričević, L.; Radivojević, A.; Živković, J. Assessment of soil erosion intensity in the Kutinska river basin in the period 1971-2016. *Fresenius Environ. Bull.* **2021**, *30*, 10890–10898.

46. De Vente, J.; Poesen, J. Predicting soil erosion and sediment yield at the basin scale: Scale issue and semi-quantitative models. *Earth-Sci. Rev.* **2005**, *71*, 95–125. [CrossRef]

47. De Vente, J.; Poesen, J.; Bazzzoffi, B.; Van Rompaey, A.; Verstraeten, G. Predicting catchment sediment yield in Mediterranean environments: The importance of sediment sources and connectivity in Italian drainage basins. *Earth Surf. Process. Landf.* **2006**, *31*, 1017–1034. [CrossRef]

48. Efthimiou, N.; Lykoudi, E.; Panagoulia, D.; Karavitis, C. Assessment of soil susceptibility to erosion using the EPM and RUSLE models: The case of Venetikos river catchment. *Glob. NEST J.* **2016**, *18*, 164–179.

49. Milevski, I. Natural hazards in the Republic of Macedonia with special emphasis on flood and earthquake in Skopje in 2016. *Geogr. Rev.* **2017**, *50*, 5–22.

50. Milevski, I.; Dragićević, S.; Radevski, I. GIS and Remote Sensing based natural hazard modeling of Kriva Reka catchment, Republic of Macedonia. *Z. Für Geomorphol.* **2017**, *58* (Suppl. S3), 213–228. [CrossRef]

51. Rakićević, T. Turbidity of rivers in the Vardar basin. In Proceedings of the Geographical Institute of the Faculty of Science and Mathematics in Belgrade, Belgrade, Serbia, 1 October 1975. (In Serbian)

52. Dimitrovska, O.; Milevski, I. Surface water quality in the Kriva Reka catchment. *Bull. Phys. Geogr. Inst.* **2005**, *2*, 109–124. (In Macedonian)
53. Milevski, I. Geomorphology of the Osogovo Mountain Massif. Ph.D. Thesis, Ss. Cyril and Methodius University in Skopje, Skopje, North Macedonia, 2006. (In Macedonian)
54. Milevski, I.; Dragićević, S.; Zorn, M. Statistical and expert-based landslide susceptibility modeling on a national scale applied to North Macedonia. *Open Geosci.* **2019**, *11*, 750–764. [CrossRef]
55. Bathrellos, G.D.; Skilodimou, H.D.; Chousianitis, K.; Youssef, A.M.; Pradhan, B. Suitability estimation for urban development using multi-hazard assess-ment map. *Sci. Total Environ.* **2017**, *575*, 119–134. [CrossRef]
56. Skilodimou, H.D.; Bathrellos, G.D.; Chousianitis, K.; Youssef, A.M.; Pradhan, B. Multi-hazard assessment modeling via multi-criteria analysis and GIS: A case study. *Environ. Earth Sci.* **2019**, *78*, 47. [CrossRef]
57. Sevieri, G.; Galasso, C.; D'Ayala, D.; De Jesus, R.; Oreta, A.; Grio, M.E.D.A.; Ibabao, R. A multi-hazard risk prioritization framework for cultural heritage assets. *Nat. Hazards Earth Syst. Sci.* **2020**, *20*, 1391–1414. [CrossRef]
58. Lombardo, L.; Tanyas, H.; Nicu, C.I. Spatial modeling of multi-hazard threat to cultural heritage sites. *Eng. Geol.* **2020**, *277*, 105776. [CrossRef]
59. Pourghasemi, R.H.; Kariminejad, N.; Amiri, M.; Edalat, M.; Zarafshar, M.; Blaschke, T.; Cerda, A. Assessing and mapping multi-hazard risk susceptibility using a machine learning techniques. *Sci. Rep.* **2020**, *10*, 3203. [CrossRef]
60. Javidan, N.; Kavian, A.; Pourghasemi, R.H.; Conoscenti, C.; Jafarian, Z.; Rodrigo-Comino, J. Evaluation of multi-hazard map produced using MaxEnt machine learning technique. *Sci. Rep.* **2021**, *11*, 6496. [CrossRef]
61. Borges, R.G.; de Assumpção, M.S.; de Almeida, M.C.F.; de Almeida, M. Seismicity and seismic hazard in the continental margin of southeastern Brazil. *J. Seism.* **2020**, *24*, 1205–1224. [CrossRef]
62. Karajovanović, M.; Hristov, S.; Jančevski, J.U.; Ivanova, V. Interpreter on the basic one Geological Map of SFRY, Kratovo and Kyustendil, 1:100,000. *Fed. Geol. Plant Belgrade* **1976**. (In Macedonian)
63. FAO. *Ground Map of the Republic of Macedonia. 1:200000*; FAO: Rome, Italy; Agricultural Institute-UKIM: Skopje, North Macedonia, 2015. (In Macedonian)
64. Petkovski, D. *Pedological Map (Interpreter): The Soils of the Area Covered by the Sheets Kyustendil 3 and 4, Kriva Palanka 1, 2, 3, 4 and Part of Kumanovo 2 and 4 on the Topographic Maps, 50k*; University "Ss. Cyril and Methodius" –Skopje, Agricultural Institute–Skopje: Skopje, North Macedonia, 2015. (In Macedonian)
65. Lazarevski, A. *Climate in Macedonia*; Misla-Skopje: Skopje, North Macedonia, 1993. (In Macedonian)
66. Copernicus. *Corine Land Cover 2018: Copernicus Land Monitoring Service*; Technical Report; Office for Official Publications of the European Communities: Luxembourgh, 2016.
67. State Statistics Office of the Republic of North Macedonia (Census 2002; 2021). Available online: www.stat.gov.mk/ (accessed on 2 April 2022).
68. Gavrilović, S. Engineering of Torrents and Erosion. *J. Constr. (Spec. Issue)* **1972**, 292. (In Serbian)
69. Dragićević, N.; Karleuša, B.; Ožanič, N. A review of the Gavrilovič method (erosion potential method) application. *Građevinar J. Croat. Assoc. Civ. Eng.* **2016**, *68*, 715–725.
70. Milevski, I. An approach of GIS-based assessment of soil erosion rate on country level in the case of Macedonia. In Proceedings of the Conference Geobalcanica, Skopje, North Macedonia, 5–7 June 2015; Volume 1.
71. Globevnić, L.; Holjević, D.; Petkovšek, G.; Rubinić, J. Applicability of the Gavrilović Method in Erosion Calculation using spatial data manipulation techniques. In *Erosion Prediction in Ungauged Basins: Integrating Methods and Techniques*; IAHS Publication: Wallingford, UK, 2003; p. 279.
72. Milanović, M.; Tomić, M.; Perović, V.; Radovanović, M.; Mukherjee, S.; Jakšić, D.; Petrović, M.; Radovanović, A. Land degradation analysis of mine-impacted zone of Kolubara in Serbia. *Environ. Earth Sci.* **2017**, *76*, 580. [CrossRef]
73. Milevski, I.; Gorin, S.; Markoski, M.; Radevski, I. Comparison of Accuracy of DEM's Available for the Republic of Macedonia. In Proceedings of the 3rd International Geographic Symposium—GEOED 2013, Antalya, Turkey, 10–13 June 2013; pp. 165–172.
74. Milevski, I. Software modeling of the intensity of recent erosion, on the example of the Kumanovo basin. In Proceedings of the II Congress of the Macedonian Geographic Society, Ohrid, North Macedonia, 3–4 October 2001; pp. 49–57.
75. Milevski, I. Factors, Forms, Assessment and Human Impact on Excess Erosion and Deposition in Upper Bregalnica Watershed (Republic of Macedonia). *Z. Für Geomorphol. Suppl. Issues* **2011**, *55* Suppl. S1, 77–94. [CrossRef]
76. Petras, J.; Holjevič, D.; Kunstek, D. Implementation of GIS-technology in Gavrilovič's method for estimation soil erosion production and sediment transport. In Proceedings of the International Conference Erosion and Torrent Control as a Factor in Sustainable River Basin Management, Belgrade, Serbia, 25–28 September 2007.
77. Karim, S. Rainfall-runoff prediction based on artificial neural network (A case study: Jarahi watershed). *Am. Eurasian J. Agric. Environ. Sci.* **2009**, *5*, 856–865.
78. Tosić, R.; Dragićević, S.; Lovrić, N. Assessment of soil erosion and sediment yield changes using erosion potential model—Case study: Republic of Srpska (BiH). *Carpathian J. Earth Environ. Sci.* **2012**, *7*, 147–154.
79. Milevski, I. Using satellite images for the analysis of recent erosion processes in the Republic of Macedonia. In Proceedings of the III Congress of MGS, Skopje, Yugoslavia, 19–22 September 2005. (In Macedonian)
80. Lazarević, R. The new method for erosion coefficient determination-Z. Erosion-Prof. *Inf. Bull.* **1985**, *13*, 54–61.

81. Blinkov, I.; Kostadinov, S. Applicability of various Erosion Risk Assessment Methods for Engineering Purposes. In Proceedings of the Conference Balwois, Ohrid, North Macedonia, 25–29 May 2010.

82. Spalević, V.; Barović, G.; Vujacić, D.; Curović, M.; Behzadfar, M.; Djurović, N.; Dudić, B.; Billi, P. The Impact of Land Use Changes on Soil Erosion in the River Basin of MiockiPotok, Montenegro. *Water* **2020**, *12*, 2973. [CrossRef]

83. Kostadinov, S.; Braunović, S.; Dragićević, S.; Zlatić, M.; Dragović, N.; Rakonjac, N. Effects of erosion control works: Case study—Grdelica Gorge, the South Morava River (Serbia). *Water* **2018**, *10*, 1094. [CrossRef]

84. Zorn, M.; Komac, B. The importance of measuring erosion processes on the example of Slovenia. *Hrvat. Geogr. Glas.* **2011**, *73*, 19–34. [CrossRef]

85. Kazimierski, L.D.; Irigoyen, M.; Re, M.; Menendez, A.N.; Spalletti, P.; Brea, J.D. Impact of climate change on sediment yield from the upper Plata basin. *Int. J. River Basin Manag.* **2013**, *11*, 411–421. [CrossRef]

86. Tavares, A.S.; Spalević, V.; Avanzi, J.C.; Alves, D. Modeling of water erosion by the erosion potential method in a pilot subbasin in southern Minas Gerais. Modelagem da erosão hídrica pelo método de erosão potencial em uma sub-bacia hidrográfica de referência no sul de Minas Gerais. *Semin. Ciências Agrárias Londrina* **2019**, *40*, 555–572. [CrossRef]

87. Ali, S.; Al-Umary, F.A.; Salar, S.G.; Al-Ansari, N.; Knutsson, S. GIS based soil erosion estimation using EPM method, Garmiyan Area, Kurdistan Region, Iraq. *J. Civ. Eng. Archit.* **2016**, *10*, 291–308.

88. Hazbavi, Z.; Azizi, E.; Sharifi, Z.; Alaei, N.; Mostafazadeh, R.; Behzadfar, M.; Spalević, V. Comprehensive estimation of erosion and sediment components using IntErO model in the Koozeh Topraghi Watershed, Ardabil Province. *Environ. Eros. Res. J.* **2020**, *10*, 92–110.

89. Behzadfar, M.; Tazioli, A.; Vukleic-Shutoska, M.; Simunic, I.; Spalevic, V. Calculation of Sediment yield in the S1-1 watershed, Shirindareh watershed, Iran. *Agric. For.* **2014**, *60*, 207–216.

90. Poornazari, N.; Khalilimoghadam, B.; Hazbavi, Z.; Bagheri Bodaghabadi, M. Land degradation assessment in the dust hotspot of southeastern Ahvaz, Iran. *Land Degrad. Dev.* **2021**, *32*, 896–913. [CrossRef]

91. Milevski, I.; Markoski, B.; Gorin, S.; Jovanovski, M. Application of Remote Sensing and GIS in Detection of Potential Landslide Areas. In Proceedings of the International Symposium Geography and Sustainable Development, Ohrid, North Macedonia, 18 April 2009; pp. 453–463.

92. Ivanova, E.; Milevski, I. Landslide Susceptibility Mapping of the Territory of Municipalities Pehčevo and Simitli by Means of GIS Modeling. In Proceedings of the Conference Space, Ecology, Safety SES, Sofia, Bulgaria, 24–26 October 2013.

93. Milevski, I.; Dragićević, S. Landslides susceptibility zonation of the territory of North Macedonia using the analytical hierarchy process approach. *Sect. Nat. Math. Biotech. Sci. MASA* **2019**, *40*, 115–126. [CrossRef]

94. Dragićević, S.; Carević, I.; Kostadinov, S.; Novković, I.; Abolmasov, B.; Milojković, B.; Simić, D. Landslide susceptibility zonation in the Kolubara River Basin (western Serbia)—Analysis of input data. *Carpathian J. Earth Environ. Sci.* **2012**, *7*, 37–47.

95. Terzaghi, K. Mechanisms of Landslides. In *Application of Geology to Engineering Practice*; Geotechnical Society of America: Berkeley, CA, USA, 1950; pp. 83–125.

96. Crozier, M. *Landslides: Causes, Consequences, and Environment*; Croom Helm: London, UK, 1986.

97. Donati, L.; Turrini, M.C. An objective method to rank the importance of the factors predisposing to landslides with the GIS methodology: Application to an area of the Apennines (Valnerina; Perugia, Italy). *Eng. Geol.* **2002**, *63*, 277–289. [CrossRef]

98. Magliulo, P.; Di Lisio, A.; Russo, F.; Zelando, A. Geomorphology and landslide susceptibility assessment using GIS and bivariate statistics: A case study in southern Italy. *Nat. Hazards* **2008**, *47*, 411–435. [CrossRef]

99. Süzen, M.; Doyuran, V. Data-driven bivariate landslide susceptibility assessment using geographical information systems: A method and application to Asarsuyu catchment, Turkey. *Eng. Geol.* **2004**, *71*, 303–321. [CrossRef]

100. Chalkias, C.; Ferentinou, M.; Polykretis, C. GIS-Based Landslide Susceptibility Mapping on the Peloponnese Peninsula, Greece. *Geosciences* **2014**, *4*, 176–190. [CrossRef]

101. He, Y.; Beighley, R.E. GIS-based regional landslide susceptibility mapping: A case study in southern California. *Earth Surf. Process. Landf.* **2008**, *33*, 380–393. [CrossRef]

102. Kumar, N.; Singh, S.K.; Pandey, H.K. Drainage morphometric analysis using open access earth observation datasets in a drought-affected part of Bundelkhand, India. *Appl. Geomat.* **2019**, *10*, 173–189. [CrossRef]

103. Durlević, U.; Novković, I.; Lukić, T.; Valjarević, A.; Samardžić, I.; Krstić, F.; Batocanin, N.; Ćurić, M.; Mijatov, M. Multihazard susceptibility assessment: A case study—Municipality of Štrpce (Southern Serbia). *Open Geosci.* **2021**, *13*, 1414–1431. [CrossRef]

104. Srejić, T.; Manojlović, S.; Sibinović, M.; Bajat, B.; Novković, I.; Milošević, M.V.; Carević, I.; Todosijević, M.; Sedlak, M.G. Agricultural Land Use Changes as a Driving Force of Soil Erosion in the Velika Morava River Basin, Serbia. *Agriculture* **2023**, *13*, 778. [CrossRef]

105. De Graff, J.V.; Romesburg, H.C.; Ahmad, R.; McCalpin, J.P. Producing landslide-susceptibility maps for regional planning in data-scarce regions. *Nat. Hazards* **2012**, *64*, 729–749. [CrossRef]

106. Wang, L.J.; Guo, M.; Sawada, K.; Lin, J.; Zhang, J. A comparative study of landslide susceptibility maps using logistic regression, frequency ratio, decision tree, weights of evidence and artificial neural network. *Geosci. J.* **2016**, *20*, 117–136. [CrossRef]

107. Saro, L.; Woo, J.; Kwan-Young, O.; Moung-Jin, L. The spatial prediction of landslide susceptibility applying artificial neural network and logistic regression models: A case study of Inje, Korea. *Open Geosci.* **2016**, *8*, 117–132. [CrossRef]

108. Liu, Q.; Yang, Z.; Shi, H.; Wang, Z. Ecological risk assessment of geo-hazards in natural world heritage sites: An empirical analysis of Bogda, Tianshan. *Open Geosci.* **2019**, *11*, 327–340. [CrossRef]

109. Srivastava, P.K.; Petropoulos, G.P.; Gupta, M.; Singh, S.K.; Islam, T.; Loka, D. Deriving Forest fire probability maps from the fusion of visible/infrared satellite data and geospatial data mining. *Model. Earth Syst. Environ.* **2019**, *5*, 627–643. [CrossRef]
110. Zhan, Y.; Fan, J.; Meng, T.; Li, Z.; Yan, Y.; Huang, J.; Chen, D.; Sui, L. Analysis of vegetation cover changes and the driving factors in the mid-lower reaches of Hanjiang River Basin between 2001 and 2015. *Open Geosci.* **2021**, *13*, 675–689. [CrossRef]